RECLAMATION
Managing Water in the West

Technical Report No. SRH-2013-15

Bedload Adaptation Length for Modeling Bed Evolution in Gravel-Bed Rivers (Interim Report)

U.S. Department of the Interior
Bureau of Reclamation
Technical Service Center
Denver, Colorado

February 2013

Mission Statements

The mission of the U.S. Department of the Interior is to protect America's natural resources and heritage, honors our cultures and tribal communities, and supplies the energy to power our future.

The mission of the Bureau of Reclamation is to manage, develop, and protect water and related resources in an environmentally and economically sound manner in the interest of the American public.

Cover Photo: August 2012 when the Upper Junction City project was under construction

Bedload Adaptation Length for Modeling Bed Evolution in Gravel-Bed Rivers (Interim Report)

Report Prepared by:

Yong G. Lai, Ph.D., Hydraulic Engineer
Sedimentation and River Hydraulics Group, Technical Service Center

David Gaeuman, Ph.D., Physical Scientist
Trinity River Restoration Division, Northern California Area Office

Peer Review Certification: This document has been peer reviewed per guidelines established by the Technical Service Center and is believed to be in accordance with the service agreement and standards of the profession. Questions concerning this report should be addressed to Timothy Randle, Group Manager of the Sedimentation and River Hydraulics Group (86-68240) at 303-445-2557.

PREPARED BY:

_____ DATE:_____
Yong Lai, Ph.D.
Hydraulic Engineer
Sedimentation and River Hydraulics Group (86-68240)

_____ DATE:_____
David Gaeuman, Ph.D.
Physical Scientist
Trinity River Restoration Division, Northern California Aerial Office

PEER REVIEWED BY:

_____ DATE:_____
Blair P. Greimann, Ph.D.
Hydraulic Engineer
Sedimentation and River Hydraulics Group (86-68240)

Table of Contents

Index of Figures

Index of Tables

Summary

Recent advances in numerical models have improved the prediction of scour, fill, bar formation, and other morphological changes in stream channels. These spatially refined numerical models attempt to account for non-equilibrium transport by incorporating an 'adaptation length' that quantifies the travel distance required for a packet of sediment to reach a new equilibrium concentration when it moves into a region of higher or lower shear stress. This project seeks to develop new models for incorporating the adaptation length for bedload transport into SHR-2D, a two-dimensional geofluvial model developed at the Technical Service Center, Reclamation.

The first task is to conduct a literature review describing existing approaches for modeling the adaptation length. The review shows that most previous attempts to deal with this issue focus on adaptation lengths for suspended sediment transport. Adaptation lengths for bedload transport, which is the mode of transport most relevant for gravel-bed rivers, have been largely neglected. The typical approach for quantifying the bedload adaptation length is to assume that it scales according to the size of dominant bedforms in the stream. Use of this type of criteria can result in estimates ranging from several times the channel width (Wu et al. 2004) to sand ripple lengths or the saltation step lengths of individual sediment grains (Phillips and Sutherland 1989; Wu et al. 2000), or even to the conclusion that the adaptation length is so small as to be negligible (Armanini 1992). In general, the values chosen by different researchers often seems to reflect differences in the types or scales of the phenomena the individual researches are most interested in as much as differences in the physical processes involved.

The second task is to identify one or more promising approaches for estimating the adaptation length that can be incorporated into SRH-2D for testing. A number of variations of a new formulation for estimating a dynamic adaptation length that varies with local hydraulics and sediment size class have been identified. First, the approach based on the theoretical equations of Seminara et al. (2002) is used as a way to compute the adaptation length implicitly. Second, a new adaptation length equation is derived based on the entrainment and deposition rate equations of Seminara et al. (2002). Finally, the saltation length equation developed by Seminara et al. (2002) is used directly as the adaptation length. In addition, a number of different sediment transport capacity equations are used to test the sensitivity of the model results to the choice of the capacity equation, along with the use of a slope dependent reference shear stress developed by Park et al. (2003).

The morphological changes at the Upper Junction City reach of the Trinity River are used as a testing case for the various approaches developed in this study. The

changes during April 2009 and August 2011 are simulated and compared with the field survey data. Numerical modeling studies find that the 2D depth-averaged geofluvial model such as SRH-2D is capable of predicting the overall erosion and deposition patterns. However, details such as pool filling are not predicted well by the model. The pool filling depth is over-predicted always. It seems difficult to predict the pool-filling processes by changing the adaptation length or sediment transport capacity equation alone. Further studies are necessary in the future to understand how to improve the prediction of riffle-pool systems.

1 Introduction

Recent advances in numerical models have improved the prediction of scour, fill, bar formation, and other morphological changes in stream channels. These numerical models are mostly multi-dimensional in nature in an attempt to resolve spatial sediment transport features longitudinally and laterally. Spatially resolved numerical models often account for non-equilibrium sediment transport by dividing sediments into multiple sizes and then tracking each size class with a separate transport equation. In addition to advection and dispersion, interactions with sediments on bed, through pickup and deposition rates, are explicitly incorporated. The pickup rate is often based on the sediment transport capacity equations that provide the equilibrium sediment concentration. For non-equilibrium transport, an 'adaptation length' (L) is used to quantify the travel distance required for a packet of sediment to reach the equilibrium concentration when it moves into a region of higher or lower shear stress. The adaptation length has been found very important by a number of previous researchers. As a result, various widely different methods have been proposed; there is, however, no consensus on an appropriate form to use. This project seeks to develop and assess new models for incorporating L for bedload transport into SHR-2D, a 2-dimensional geofluvial model developed at the Technical Service Center, Bureau of Reclamation.

2 Approaches

In the existing SRH-2D model, each sediment size class k is governed by a separate transport equation expressed as follows:

$$\frac{\partial hC_k}{\partial t} + \frac{\partial \cos(\alpha_k)\beta_k V_t hC_k}{\partial x} + \frac{\partial \sin(\alpha_k)\beta_k V_t hC_k}{\partial y} =$$

$$\frac{\partial}{\partial x}\left(hf_k D_x \frac{\partial C_k}{\partial x}\right) + \frac{\partial}{\partial y}\left(hf_k D_y \frac{\partial C_k}{\partial y}\right) + S_{e,k} \tag{1}$$

Variou terms of the above equation may be found in Greimann et al. (2008). It is sufficient to point out that the source term $S_{e,k}$ represents the effect of sediment pick up and deposition rates and is expressed as:

$$S_{e,k} = E_k - D_k = \frac{1}{L_{t,k}}(q_{t,k}^* - \beta_k V_t hC_k) \tag{2}$$

In the above, E_k is the pickup rate, D_k is the deposition rate, $q_{t,k}^*$ is the equilibrium or capacity sediment transport rate, and $L_{t,k}$ is the adaptation length. Equation (2) is in the form of total load; it recovers to forms for purely suspended load and bed load as follows:

$$S_{e,k} = \begin{cases} \zeta_k \omega_{s,k}(C_{s,k}^* - C_{s,k}) & for\ suspended\ load \\ \dfrac{1}{L_{b,k}}(q_{b,k}^* - q_{b,k}) & for\ bed\ load \end{cases} \tag{3}$$

For gravel beds, we are dealing with bed load transport only.

The first task of this project is to complete a literature review describing existing approaches for modeling the adaptation length. The study shows that most previous attempts to deal with this issue focus on adaptation lengths for suspended sediment transport. Adaptation lengths for bedload transport, which is the mode of transport most relevant for gravel-bed rivers, have been largely neglected.

Typical approaches for addressing purely suspended load transport are described by authors such as Armanini and Di Silvio (1988), Armanini (1992), Wang and Wu (2004), and Wu (2004) in generally similar ways. Typically, the adaptation length was expressed as a function of particle fall velocity and a sediment

exchange rate paramter. This type of approach is inappropriate for bedload transport.

The typical approach for quantifying L for bedload is to assume that it scales according to the size of dominant bedforms in the stream. Use of this type of criteria can result in estimates ranging from several times the channel width or dune or bar length (Wu et al. 2004) to sand ripple lengths (Thuc, 1991) or the saltation step lengths of individual sediment grains (Phillips and Sutherland 1989; Wu et al. 2000), or even to the conclusion that L is so small as to be negligible (Armanini 1992). Some even suggested the use of multiple times of the mesh size (Rahuel et al., 1989). In general, the values chosen by different researchers often seem to reflect differences in the types or scales of the phenomena the individual researches are most interested in as much as differences in the physical processes involved.

The second task of this project is to identify a few promising approaches for estimating the adaptation length that can be incorporated into SRH-2D for testing. Two variations of a new formulation for estimating a dynamic adaptation length that varies with local hydraulics and sediment size class have been identified. The approach is based on the theoretical equations quantifying sediment entrainment and deposition rates presented by Seminara et al. (2002). The rates at which bedload particles of a grain size k are entrained (E_k) and deposited (D_k) are given by Seminara et al. (2002) as:

$$\frac{E_k}{\sqrt{(s-1)gd_k}} = \alpha\left(\theta_k - \theta_{k,c}\right)^{3/2} \tag{4a}$$

$$\frac{D_k}{\sqrt{(s-1)gd_k}} = \beta\left(\theta_k - \theta_{k,c}\right)^{1/2}\xi_k^* \tag{4b}$$

Here, s is the specific weight of the sediment, g is gravitational acceleration, α and β are numerical constants equal to 0.0199 and 0.03, respectively, $\theta_k = \tau_b / \left[\rho g(s-1)d_k\right]$ is the Shield's parameter of sediment size class k, and ξ_k^* is a dimensionless bedload concentration, given by:

$$\xi_k^* = \frac{hC_k}{d_k} \tag{5}$$

The above entrainment and deposition rates are directly implemented in SRH-2D. This approach essentially produces a new sediment transport capacity equation that is solved numerically and the effect of adaptation length is taken into account implicitly.

The Seminara et al. (2002) equations may also be used to derive a new adaptation length expression. The entrainment and deposition rates may be transformed into the following form:

$$S_{e,k} = E_k - D_k = \frac{1}{L_{b,k}} \left(q_{b,k}^* - q_{b,k} \right) \tag{6a}$$

$$q_{b,k}^* = \frac{\alpha}{\beta} V_s d_k \left(\theta_k - \theta_{k,c} \right) \tag{6b}$$

$$q_{b,k} = V_s h C_k \tag{6c}$$

$$L_{b,k} = \frac{V_s d_k}{\beta \sqrt{(s-1)g d_k} \sqrt{\theta_k - \theta_{k,c}}} = \frac{V_s d_k}{\beta \sqrt{(\tau_b - \tau_{cri})/\rho}} \tag{6d}$$

In the above, $V_s = \beta_k V_t$ is the sediment movement velocity, $q_{b,k}^*$ is the transport capacity rate, and $L_{b,k}$ is the bedload adaptation length. Equation (6d) is a new bedload adaptation length that is implemented in SRH-2D and is used together with other sediment capacity equations.

In addition, the study of Seminara et al. (2002) determined that the bed load adaptation length might be computed as:

$$L_{b,k} = 286.4 d_k \tag{7}$$

Equation (7) is the third option used to test out the bedload adaptation length options.

For riffle-pool modeling, it is recognized that entrainment parameters may vary with bed slope. An analysis was performed by Parker et al. (2003) to consider the variation of critical shear stress for entrainment with local bed slope. According to Paker et al. (2003), the ratio of the critical shear stress on a slope to that on a flat surface, $X = \frac{\theta_{k,c}}{\theta_{k,c,flat}}$, may be computed from the following quadratic relation:

$$(1-\Delta)X^2 + 2.0BX - C = 0 \tag{8a}$$

$$\Delta = \frac{4}{3} \mu \frac{c_L}{c_D} r_L \tag{8b}$$

$$B = \frac{\Delta}{\sqrt{1 + \tan^2 \alpha + \tan^2 \varphi}} + \frac{\sin \alpha}{\mu} \tag{8c}$$

$$C = \frac{1+\Delta}{1 + \tan^2 \alpha + \tan^2 \varphi} \left(1 - \frac{\tan^2 \alpha + \tan^2 \varphi}{\mu^2} \right) \tag{8d}$$

So the final ratio may be computed by:

$$\frac{\theta_{k,c}}{\theta_{k,c,flat}} = \frac{\sqrt{B^2 + (1-\Delta)C} - B}{1-\Delta} \tag{9}$$

In the above, Δ is a parameter quantifying the lift force from 0 to 1 (0.587 may be used by default), $\mu = \tan(\phi_a)$ with ϕ_a the angle of repose (35 deg may be used), α is the bed angle along the sediment movement direction, and φ is the bed angle along the line normal to the sediment direction.

Finally, the sediment transport capacity equation is important in predicting morphological changes. In addition to the Seminara et al. (2002) equation discussed above, other capacity equations are also used in this study. They include both the Wilcock-Crown (2003) equation and the Trinity capacity equation developed by Gaeuman et al. (2009). Both equations may be expressed for sediment size class k as:

$$\frac{q_{t,k}^* g(s-1)}{(\tau_b/\rho_w)^{1.5}} = p_{ak}G(\phi_k); \qquad \phi_k = \frac{\theta_k}{\theta_r}\left(\frac{d_k}{d_{50}}\right)^{\alpha_k} \tag{10}$$

In the above, $q_{t,k}^*$ is the volumetric sediment transport rate per unit width, p_{ak} is the volume fraction of sediment size class k on the bed, $s = \rho_S/\rho_w$, ρ_w and ρ_S are the water and sediment density, respectively, g is the gravitational acceleration, τ_b is bed shear stress, $\theta_k = \tau_b/[\rho_w g(s-1)d_k]$ is Shield's parameter of sediment size class k; θ_r is the reference Shield's parameter, d_k is diameter of sediment size class k, and d_{50} is the median diameter of the sediment mixture in bed. The function in the transport equation is expressed as:

$$G(\phi) = \begin{cases} 14.0(1 - 0.894/\phi^{0.5})^{4.5} & \phi \geq 1.35 \\ \\ 0.002\,\phi^{7.5} & \phi < 1.35 \end{cases} \tag{11}$$

Two parameters must be defined to apply the above equation: θ_r and α_k. The parameter θ_r is a reference value above which sediment is mobilized and α_k is the exposure or hiding factor to account for reduction in critical shear stress for larger particles and increase in critical shear stress for smaller particles. The standard Trinity capacity equation used the following values in SRH-2D:

$$\theta_r = 0.021 + 0.0155\exp(-20F_s) \tag{12a}$$

$$\alpha_k = 1 - \frac{0.7}{1 + \exp(1.9 - d_k/3d_{50})} \tag{12b}$$

where F_s is the fraction of sand on the bed surface (the cutoff diameter of the "sand" may range from 1 to 4 mm). In this study, a constant reference value of $\theta_r = 0.035$ is used. The Wilcock-Crowe (2003) capacity equation used the following default values:

$$\theta_r = 0.021 + 0.015 \exp(-20F_s) \qquad (13a)$$

$$\alpha_k = 1 - \frac{0.67}{1 + \exp(1.5 - d_k / d_{50})} \qquad (13b)$$

3 Case Description

A Trinity River reach near the Upper Junction City (UJC) is selected to test and validate the various adaptation length methods, as well as other modeling parameters discussed above. This section describes the test case itself.

3.1 Terrain Data

The bathymetry and topography of the UJC reach selected for model tests were obtained by engineers of TRRP. Two sets of data were obtained from various survey methods under the existing condition: one 2009 data set and another 2011 data set. The two sets of terrain data are displayed in Figure 1 and Figure 2, respectively, along with the aerial photos.

The 2009 terrain incorporates data from two sources. Terrestrial and bathymetric LiDAR was flown in early April 2009 before flow started going up for the 2009 release. This data was very good in the emergent areas but poor in the shallow submerged areas. Therefore, sonar data was obtained in areas deeper than about a meter in November to December of 2009. The sonar is in the pools and other deeper areas in the more upstream of the two big bends in the model. The exact dates aren't that important because the only time flows were high enough to move gravel around or erode the banks was during the 2009 release – late April through June or early July. The winter floods didn't come until after the sonar was collected.

The 2011 terrain was updated using ground survey data collected on October 4, 2011 along the eroding part of the bank and in the wadable part of the channel where that big bar complex is depositing adjacent to where the bank has eroded a lot (lower half of the site). Additional sonar was conducted on July 7, 1011 in the deeper areas in the upstream bend and through the cross over. The shallow area where the wide bar is near the bridge was covered with a ground survey on Sept. 26 and 27, 2011. Again, nothing much happens between the spring release and the winter storms that usually don't come until late December or January.
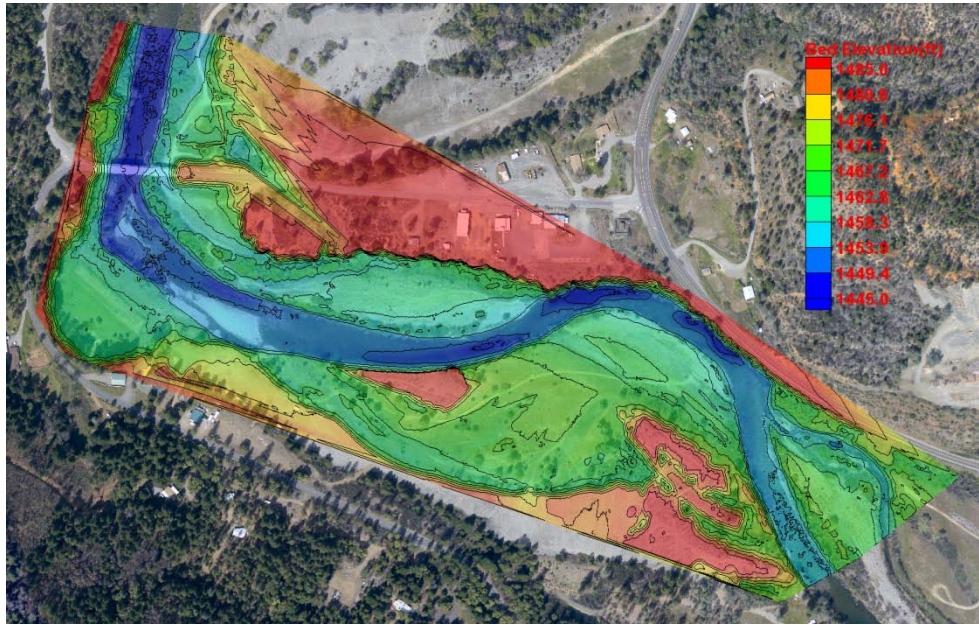
Figure 1. Terrain based on 2009 survey data under the existing condition (aerial photo is in April, 2009)
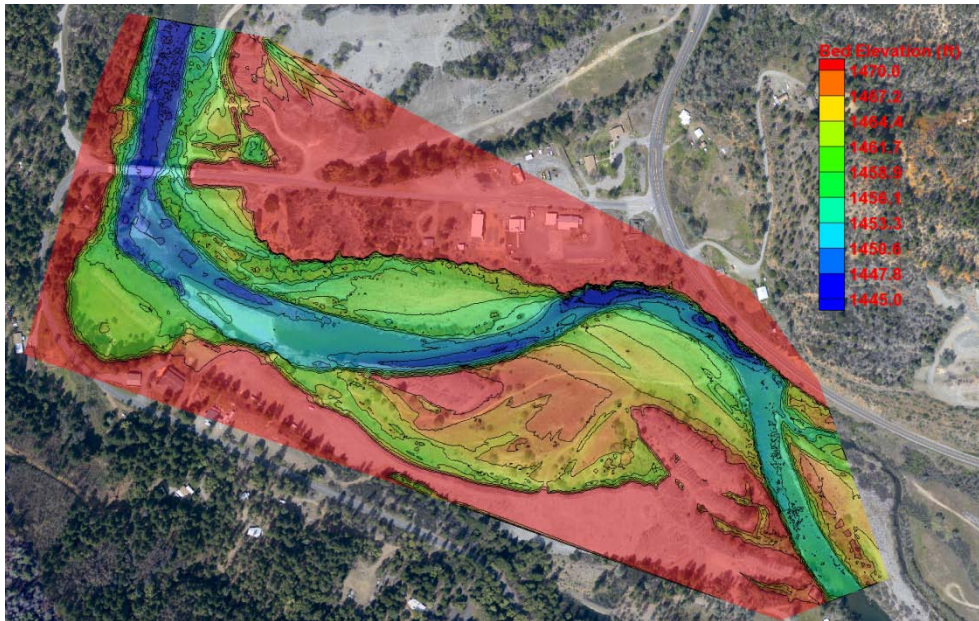
Figure 2. Terrain based on 2011 survey data under the existing condition (aerial photo is in April, 2009)

3.2 Bank Data

A total of ten banks along the study reach, named UJC-A through UJC-J, were selected by Cardno ENTRIX for both field and BSTEM modeling studies (Cardo ENTRIX, 2012). The locations of the ten banks are shown in Figure 3.
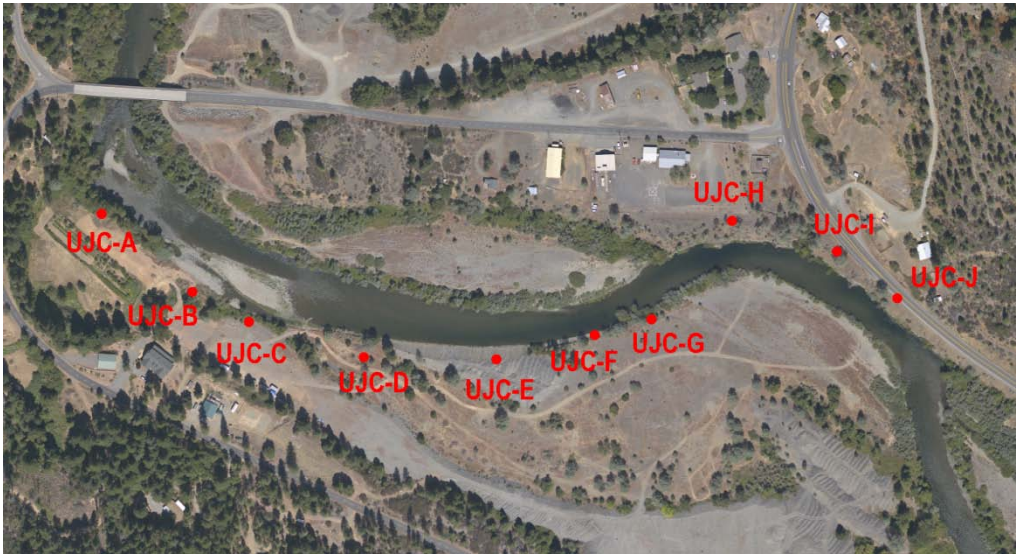
Figure 3. Locations of ten banks where field survey and BSTEM modeling were carried out by Cardno ENTRIX

For the coupled geofluvial modeling with SRH-2D and bank erosion module, some bank properties are needed as model inputs. Based on the bank retreat data derived from the difference between the 2009 and 2011 terrain data, the section of the left bank selected for a coupled modeling encompasses banks UJC-C to UJC-F (see Figure 3). The bank properties at these four bank locations are tabulated in Table 1 through Table 4; they are based on the BSTEM input files prepared by the Cardno ENTRIX study (Cardno ENTRIX, 2012). These properties were from field measurement and BSTEM calibration study.

Table 1. Bank properties at UJC-C site

Bank Layer	Thickness (m)	Critical Shear Stress (Pa)	Erodibility (cm^3/Ns)	Saturated unit weight (kN/m^3)	Friction angle ϕ'	Cohesion c' (kPa)	ϕb	
1	2.6	15.07	0.17	20	36	1	15	
2	2.0	15.07	0.17	20	36	1	15	
3	2.0	15.07	0.17	20	36	1	15	
All three layers have the same following composition (diameter in mm)								
<0.5	0.5-1.41	1.41-2	2-4	4-8	8-16	16-32	32-64	>64
0	4	4	4	6	18	50	75	100

Table 2. Bank properties at UJC-D site

Bank Layer	Thickness (m)	Critical Shear Stress (Pa)	Erodibility (cm^3/Ns)	Saturated unit weight (kN/m^3)	Friction angle ϕ'	Cohesion c' (kPa)	ϕb	
1	0.9	0.71	2.123	18	32	.4	15	
2	0.75	0.71	2.123	18	32	.4	15	
3	0.75	0.71	2.123	18	32	.4	15	
4	0.75	0.71	2.123	18	32	.4	15	
All three layers have the same following composition (diameter in mm)								
<.0025	.0025 -.088	.088 -0.25	0.25 -0.354	0.354 -0.5	0.5 -1.41	1.41 -2	2 -4	>4
2.5	6	9.9	27	57	84	94	100	100

Table 3. Bank properties at UJC-E site

Bank Layer	Thickness (m)	Critical Shear Stress (Pa)	Erodibility (cm^3/Ns)	Saturated unit weight (kN/m^3)	Friction angle ϕ'	Cohesion c' (kPa)	ϕb
1	3	23.81	0.117	20	36	.4	15
2	3	23.81	0.117	20	36	.4	15
3	3	23.81	0.117	20	36	.4	15
4	3	23.81	0.117	20	36	.4	15
All three layers have the same following composition (diameter in mm)							
<0.5	0.5-4	4-8	8-16	16-32	32-64	>64	
0	1	2	10	32	57	100	

Table 4. Bank properties at UJC-F site

Bank Layer	Thickness (m)	Critical Shear Stress (Pa)	Erodibility (cm^3/Ns)	Saturated unit weight (kN/m^3)	Friction angle ϕ'	Cohesion c' (kPa)	ϕb
1	0.6	7.78	0.294	20	36	0	15
2	1.95	7.78	0.294	20	36	0	15
3	1.95	20.9	0.13	20	36	0	15
4	1.5	20.9	0.13	20	36	0	15
5	1.5	75.33	0.045	20	36	0	15

Layer 1 & 2 composition (diameter in mm)

<.002	.002-.063	.063-.354	.354-.5	0.5-1.41	1.41-2	2-16	16-32	32-64	>64
0	1.19	6.19	14.23	23.21	31.24	46	62	83	100

Layer 3 & 4 composition (diameter in mm)

<.002	.002-.063	.063-.354	.354-.5	0.5-1.41	1.41-2	2-16	16-32	32-64	>64
0	0.55	3.48	6.73	11.15	15.53	25	35	62	100

Layer 5 composition (diameter in mm)

<0.5	0.5-16	16-32	32-64	>64
0	4	5	14	100

4 Numerical Model Description

4.1 About SRH-2D

SRH-2D version 3, Sedimentation and River Hydraulics – Two-Dimensional, is used for the current modeling study. SRH-2D is a 2D depth-averaged hydraulic and sediment transport mobile-bed model for river systems. It is developed at the Technical Service Center, Bureau of Reclamation. The hydraulic flow model, documented by Lai (2008; 2010), is widely used by internal and external users. The sediment transport mobile-bed model, used to predict stream bed vertical change, is still under development. The mobile-bed model has been applied to a wide range of projects at Reclamation since 2008. The mobile-bed model theory and selected results may be found in Greimann et al. (2008), Lai and Randle (2007), Lai and Greimann (2008; 2010) and Lai et al. (2011). At present, a beta-version has been distributed to selected external users.

The robustness and reliability of SRH-2D have been proven with a wide range of Reclamation projects as well as with studies at external institutions. Detailed technical information of SRH-2D and selected application cases may be downloaded from the following Reclamation website: http://www.usbr.gov/pmts/sediment/. Some of the unique features of SRH-2D have been discussed by Lai (2008). A primary feature is the use of a flexible mesh. The arbitrarily shaped element method of Lai et al. (2003) is adopted for geometry representation. This essentially allows the use of most existing meshes available: structured quadrilateral mesh, purely triangular finite element mesh, Cartesian mesh, or hybrid mesh. Our experience shows that the hybrid mesh, in which a combination of quadrilateral meshes along main channel and triangular meshes in the remaining zones is used, is most flexible. It often leads to increased accuracy and efficiency. Other important features include the relatively stable numerical algorithms used with very few stability-ensuring parameters and ease of use of the model.

Major modeling capabilities of SRH-2D are as follows:

- 2D depth-averaged governing equations with the dynamic wave (shallow water) approximation for flow hydraulics;
- An implicit solution scheme for time advancement;
- Unstructured meshes with arbitrary mesh cell shapes. In most applications, a combination of quadrilateral and triangular meshes is recommended;
- Steady or unsteady flows;
- Subcritical, supercritical or transcritical flow regimes;
- Time-accurate, non-equilibrium modeling of sediment transport;
- Multi-size-class sediment transports with bed sorting and armoring;

- A unified formulation for suspended load, bedload and mixed load;
- Effects of gravity and secondary flows;
- Non-cohesive or cohesive sediments; and
- Coupled mobile-bed and bank erosion modeling.

SRH-2D is a 2D model; it is particularly useful for problems where 2D effects are important. Examples include flows with in-stream structures such as weirs, diversion dams, release gates, coffer dams, etc.; bends and point bars; perched rivers; and multi-threaded streams. 2D models may also be needed if some flow features are important such as flow recirculation and eddies, lateral variations, overtopping over banks and levees, differential flow shears on river banks, and interactions between the main channel, vegetated areas and floodplains. Some of the scenarios listed above may be modeled by 1D models. However, additional empirical sub-models need to be supplemented and extra calibrations must be carried out with unknown uncertainties.

4.2 Model Setup Details

SRH-2D modeling, in general, includes the following steps:

(1) Selection of the solution domain;
(2) Mesh generation for the solution domain;
(3) Topography, flow roughness, and bed sediment gradation representation;
(4) Model calibration; and
(5) Model applications.

The first three steps are discussed below.

4.2.1 Solution Domain, Mesh and Zonal Representation

A 2D analysis begins by defining a solution domain and then generating a mesh that covers the domain. The solution domain may be determined based on the objectives of the project, the area of interest for the project study questions, and the upstream and downstream channel forms. The domain may also be constrained by available survey data due to the high cost of bathymetric and topographic surveys. In this study, the solution domain is mostly limited by the available terrain data.

The solution domain selected is displayed in Figure 4. It encompasses about 4,000 ft in channel longitudinal length and an average of 700 ft in width.

The mesh is generated within the solution domain using the Surface-water Modeling System software (SMS). The following website link provides more information about SMS: http://www.aquaveo.com. Additionally, the SRH-2D manual (Lai, 2008) may be consulted for an in-depth discussion on how to generate an appropriate 2D mesh. The mesh consists of mixed quadrilaterals and triangles with a total of 18,414 mesh cells (see Figure 4). The 2009 terrain data is

used to obtain bed elevation at each mesh point. The terrain represented by the mesh is displayed in Figure 5.
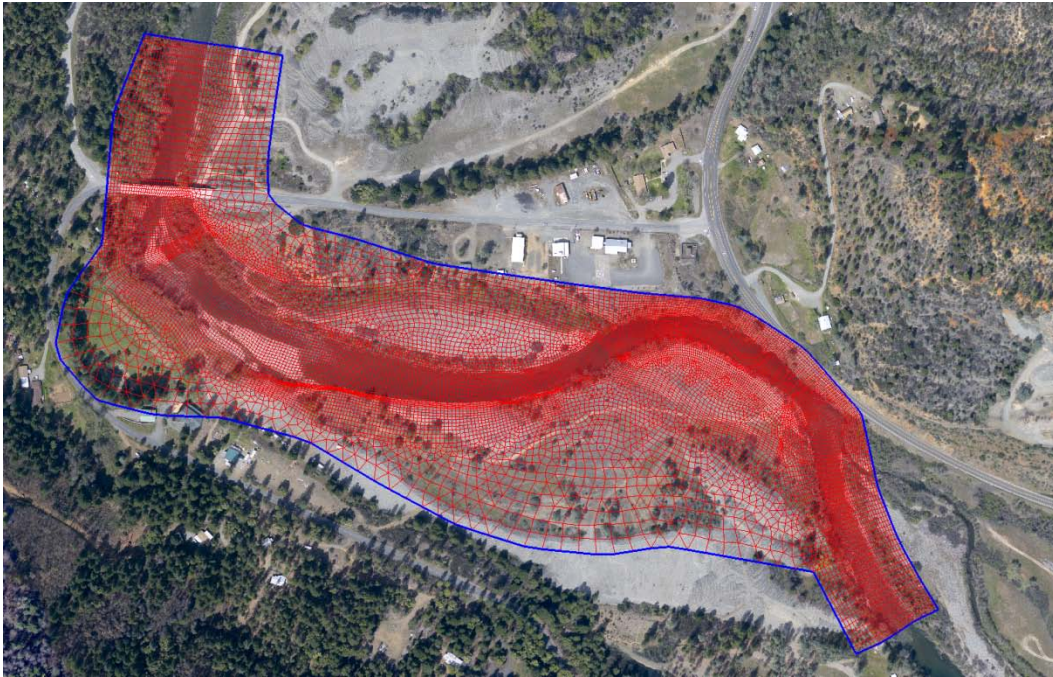

Figure 4. Solution domain (blue) along with the mesh (red) used for the geofluvial modeling (aerial photon in April, 2009)
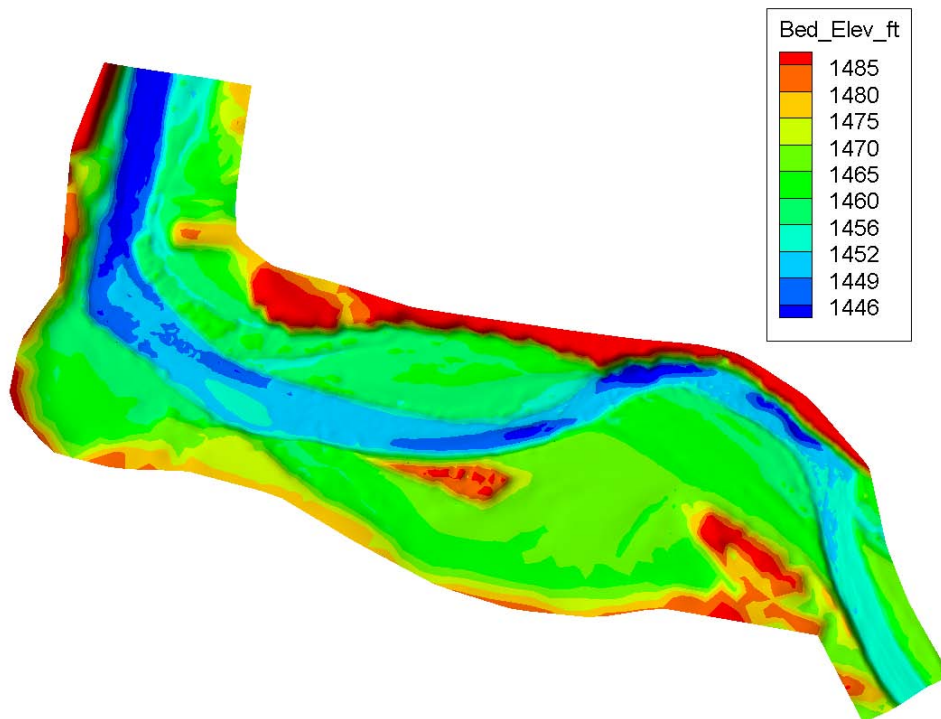

Figure 5. 2009 terrain represented by the mesh

Flow resistance is computed with the Manning's roughness equation in which the Manning's coefficient (n) is used as one of the model inputs. The Manning's coefficient may be estimated from the field, based on previous studies on the same or similar rivers, or calibrated using the measured water surface elevation data. In this study, it is estimated from the previous studies on the Trinity River. The solution domain is divided into three zones as shown in Figure 6. The Manning's coefficient for each zone is assigned with the following values: 0.035 for the main channel and the bare floodplain and 0.085 for the vegetation zone.
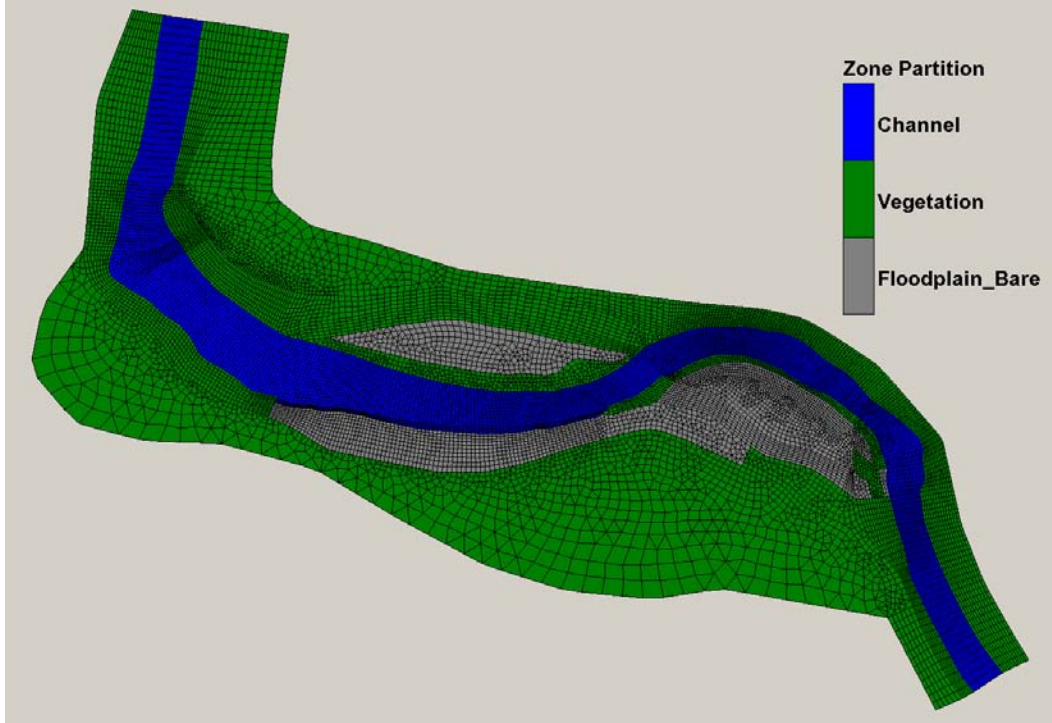

Figure 6. Zonal partition of the solution domain for both roughness assignment and bed gradation representation

The bed sediment gradation over the solution domain is also needed for the mobile bed vertical erosion modeling. The bed gradation is represented by the same zonal partition in Figure 6. The bed sediment in the main channel is divided into two layers. The top layer has about 0.65 ft thickness while the bottom layer has infinite thickness. The bed gradations of each layer are based on survey data and are plotted in Figure 7. The gradations are almost the same for the two layers with a medium diameter (d_{50}) of about 29 mm. The bare floodplain is assumed to have the uniform sediment gradation that is the same as the bottom layer of the main channel. In the vegetated zone, only deposition is allowed and therefore, no bed gradation is needed by the model.
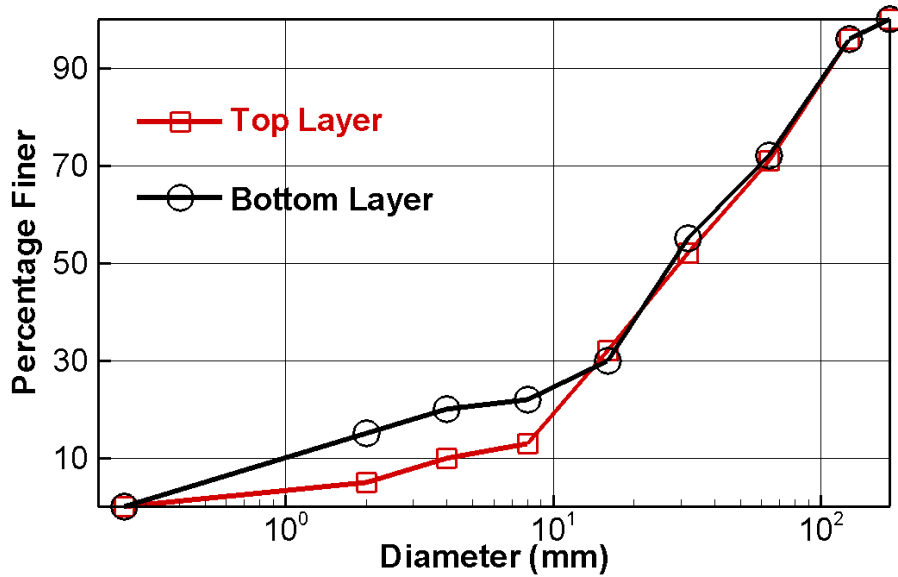
Figure 7. Bed sediment gradation distribution

4.2.2 Boundary Conditions and Other Model Inputs

Time-accurate unsteady simulations have been carried out using the hydrograph from April 29, 2009 to September 3, 2011 (USGS gaging station 11526250) that covers three spring runoffs. The daily flow hydrograph is shown in Figure 8. Only discharges above a pre-selected value are used for mobile bed modeling. It is done for two reasons: (1) only large flows mobilize stream bed and change stream morphology, and (2) computing time may be reduced significantly by ignoring the smaller flows. The cutoff discharge value used in this study is 2,000 cfs. The time series discharges after removal of those below the cutoff discharge is displayed in Figure 9. The total simulation is reduced to about 22% of the original time with the 2,000cfs cutoff value.

The potential impact of the cutoff discharge may be estimated by computing the Shields parameter at the cutoff discharge. For the 2,000 cfs discharge, the Shields parameter based on the reference diameter of 29 mm is shown in Figure 10. The results show that the discharge of 2,000 cfs may mobilize sediments in a few areas. However, no appreciable changes of channel morphology are expected at this flow.
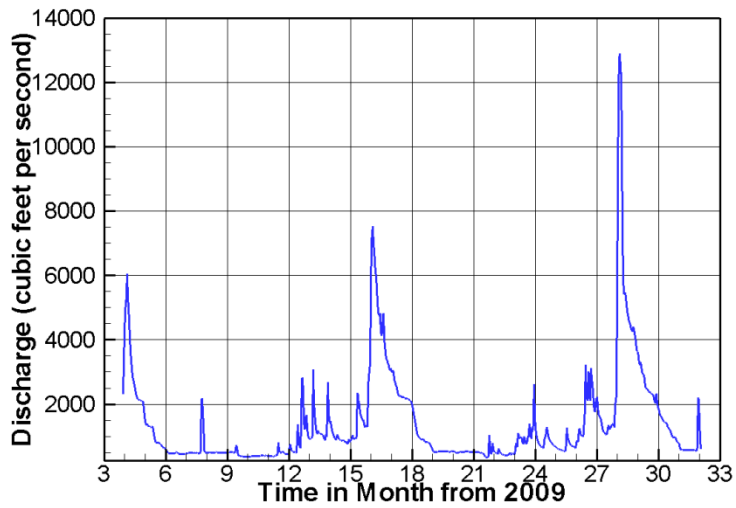
18

Figure 8. Daily flow discharge from April 29, 2009 to September 3, 2011 at the Upper Junction City site
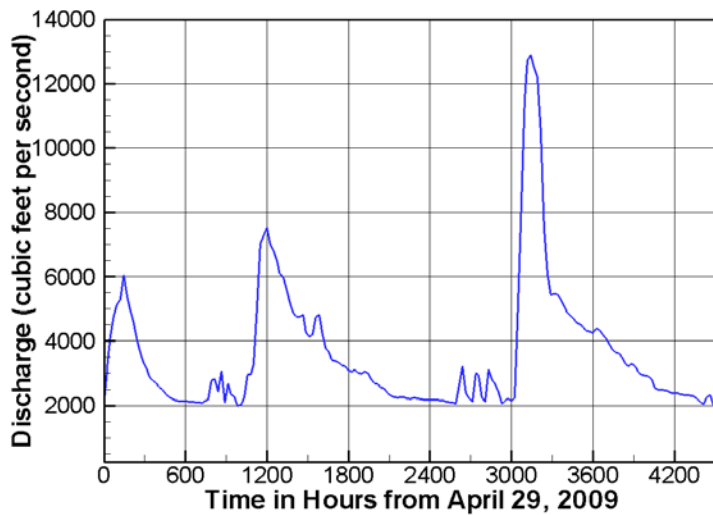

Figure 9. Daily flow discharge at the Upper Junction City after removal of smaller discharges below 2,000 cfs
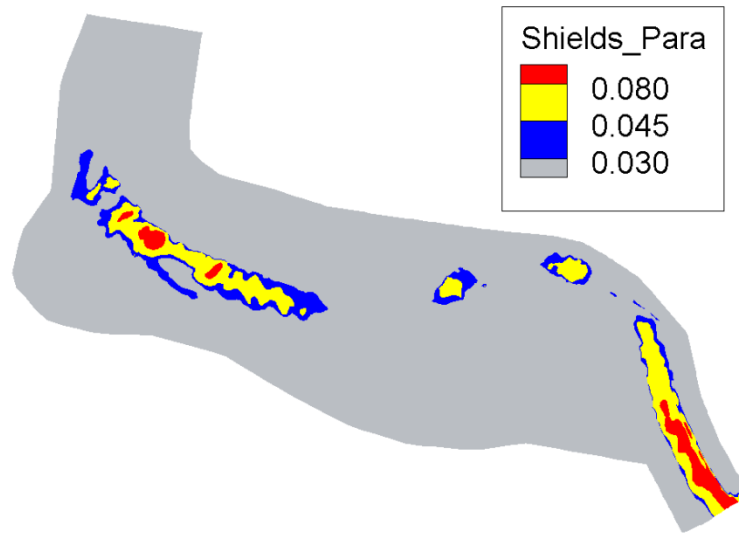
Figure 10. Shields parameter distribution under a constant flow of 2,000 cfs and a reference sediment diameter of 29 mm

Sediment load is needed as another upstream boundary condition. In this study, the sediment rating curves developed by engineers at TRRP, based on the 2006-2007 sediment data at the Douglas City site of the Trinity River, are used. They are plotted in Figure 11. It is noted that the two largest size classes (above 64 mm) have higher sediment rates than those of the smaller ones (2-32 mm range) once the flow is higher than 7,000 cfs.
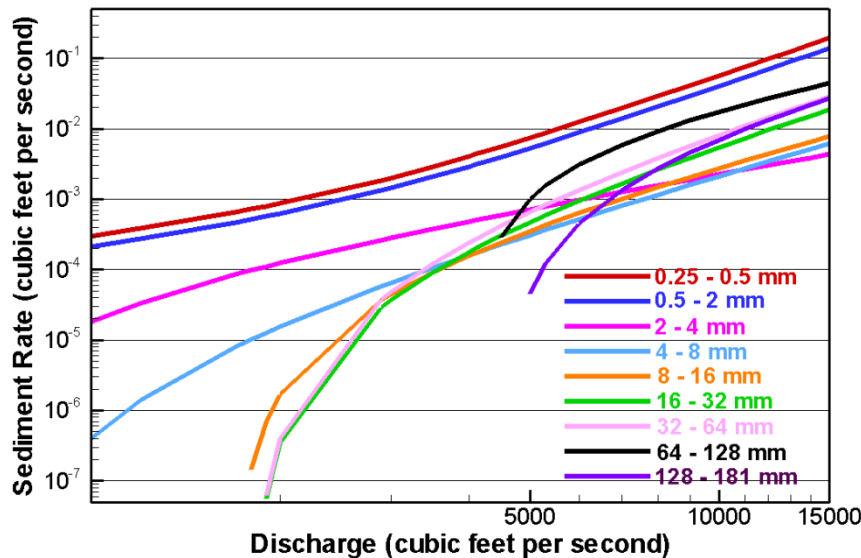

Figure 11. Sediment rate rating curves for various sediment size classes at the upstream boundary

20

Water surface elevation (stage) at the downstream boundary is needed as the downstream boundary condition. A stage-discharge rating curve was generated using HEC-RAS model by TRRP and is used as shown in Figure 12.
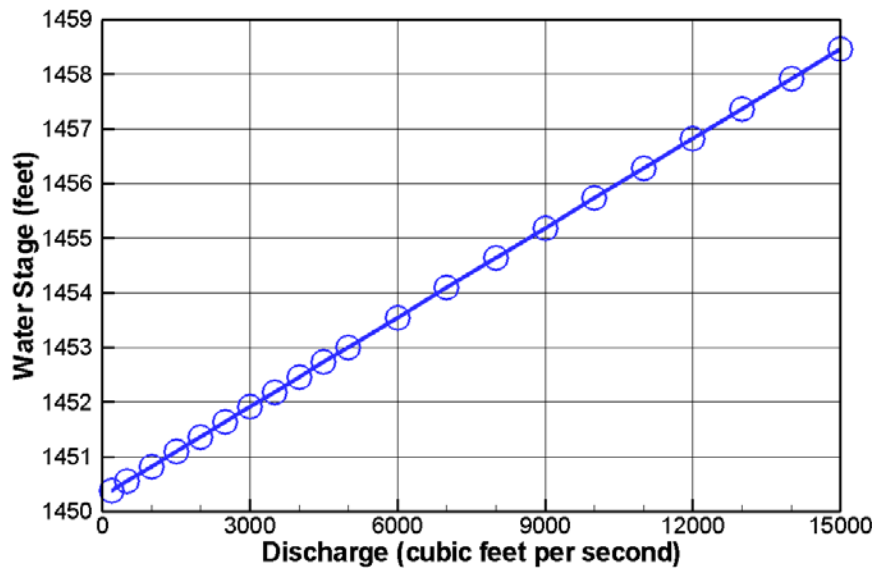

Figure 12. Stage-discharge rating curve, obtained with HEC-RAS, at the downstream boundary

A total of nine sediment size classes are used to represent bed material load and the partition is tabulated in Table 5.

Table 5. Size ranges of all sediment size classes

| Sediment Size Class	Size Range (mm)
1	0.25 to 0.5
2	0.5 to 2
3	2 to 4
4	4 to 8
5	8 to 16
6	16 to 32
7	32 to 64
8	64 to 128
9	128 to 181

Other model inputs include the following. The time step is 5 seconds and it is used mostly for numerical stability control. The active layer thickness is chosen to be 0.15 ft, about five times d_{50} and 1.5 times d_{90}. The bedload adaptation length and sediment transport capacity equation are varied in this study and are presented in the results section.

4.2.3 Bank Erosion Parameters

The left bank section simulated with the coupled SRH-2D and bank erosion module is shown in Figure 13. The input data for bank erosion modeling are based on the surveyed banks UJC-C through UJC-F presented in Section 2.2. The time step for the bank module is six hours.

A total of sixteen cross sections are used for bank retreat modeling (see Figure 14); they are coupled to the SRH-2D modeling. Each bank cross section is assumed to have uniform materials and properties and is simulated as a non-cohesive bank. Therefore, the linear retreat bank erosion module is used in this study. This decision is based on the bank data in Section 2.2. With the linear retreat module, the measured critical shear stress and erodibility are the key inputs to compute bank retreat; the geotechnical failure modeling offered by BSTEM is not used. Instead, bank failure is determined by the angle of repose approach.

The eroded sediments from banks are added back to the stream according to the user-supplied deposition zones shown in Figure 15. It is implemented as follows: eroded bank sediments from banks touching the deposition zone, say i, are added to zone i mesh cells uniformly. The portion of the 2D mesh that includes the retreating bank is moved and deformed while banks are retreating. Users have the option to specify the moving mesh zone and it is as shown in Figure 16 in this study.
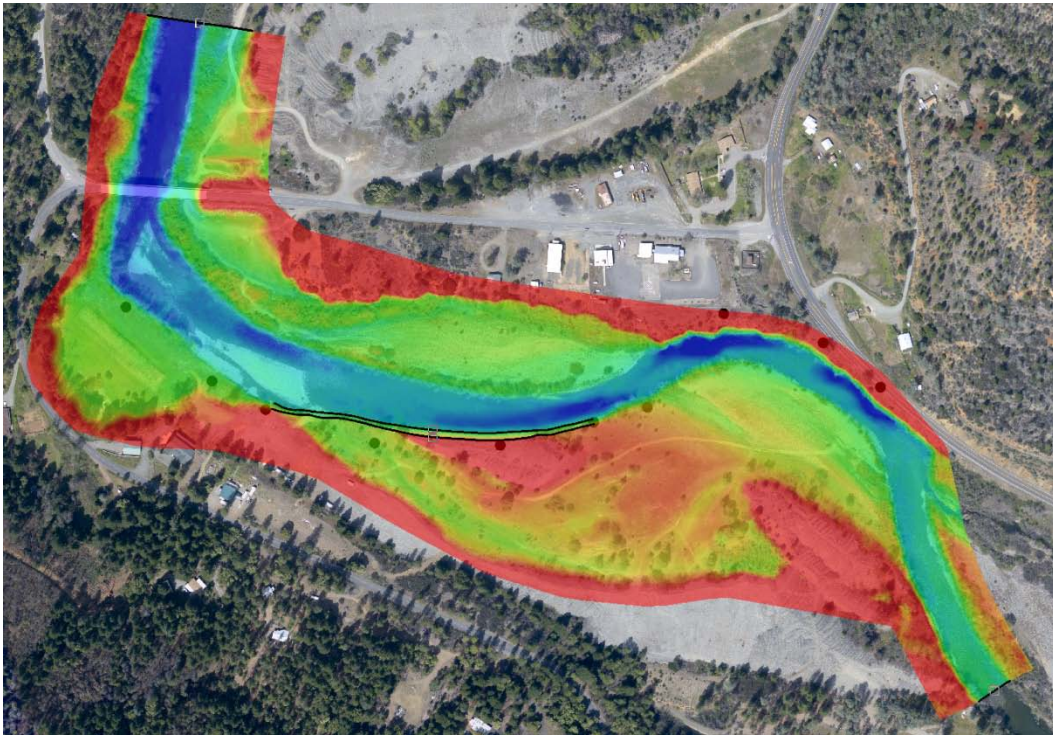
(a) Overall View
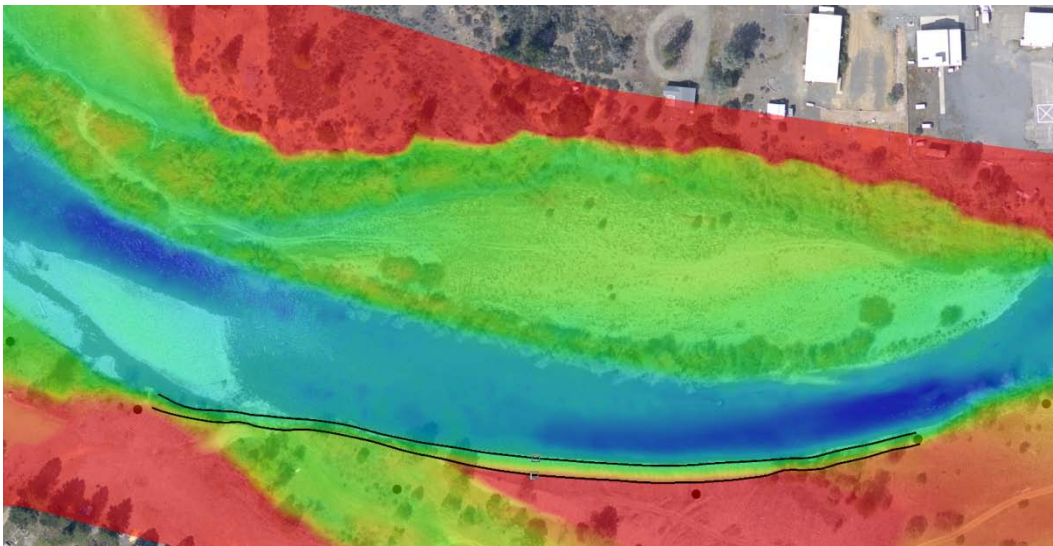
(b) A Zoom-In View

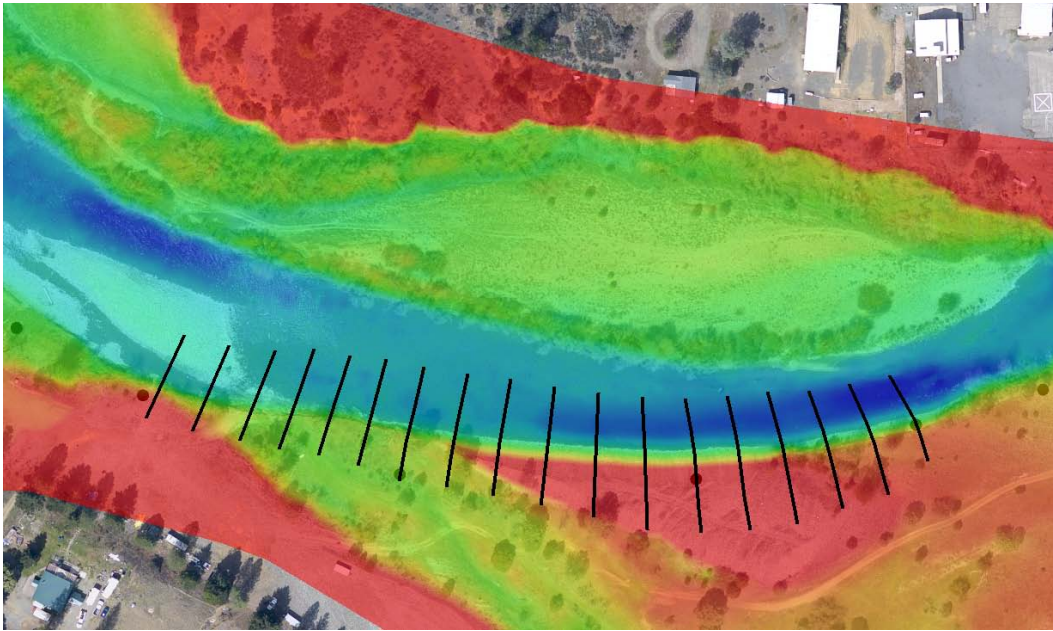Figure 13. The bank section (black lines) that is subject to bank erosion modeling

Figure 14. Bank cross sections (black lines) used for a coupled modeling between SRH-2D and bank erosion module
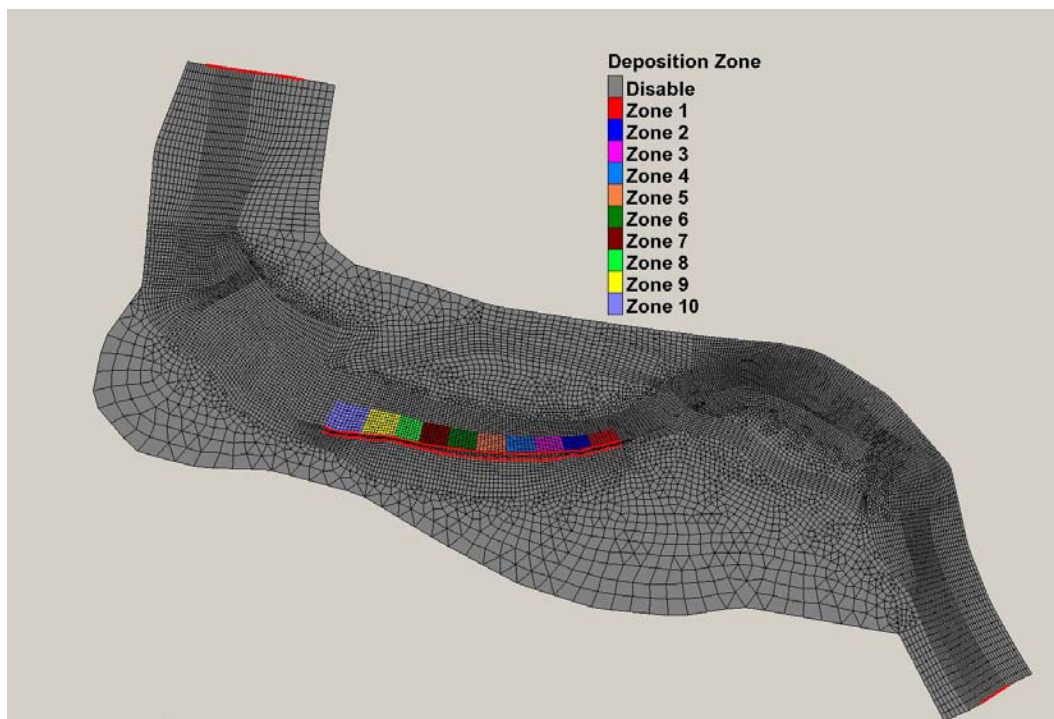

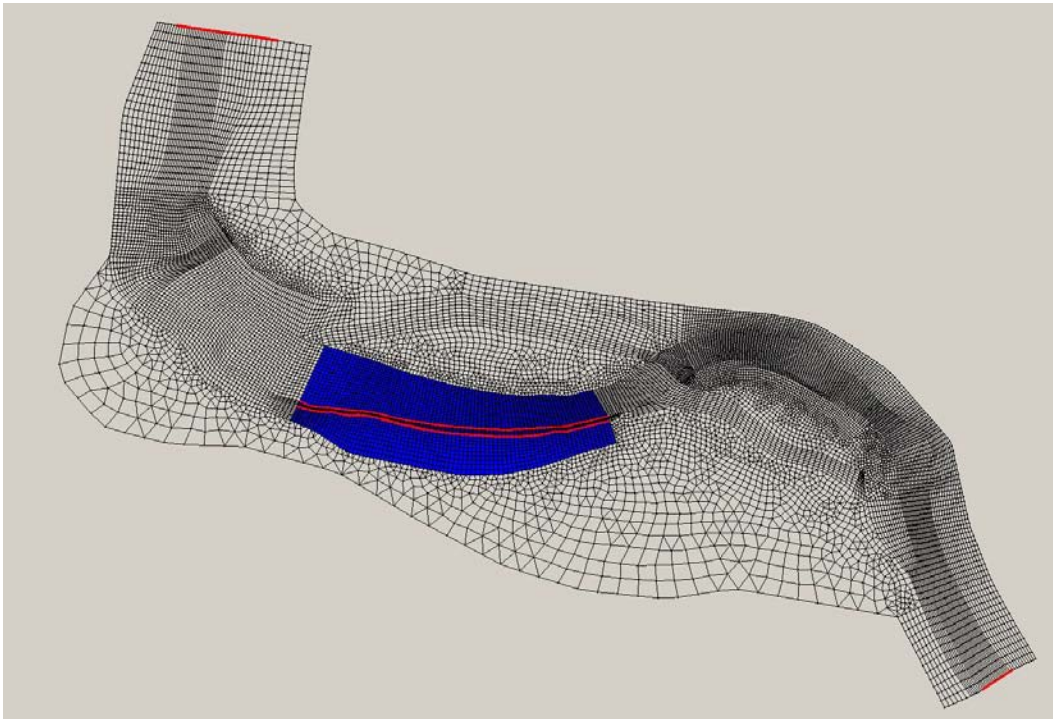Figure 15. Deposition zones for the eroded bank materials

Figure 16. The mesh within the blue area is moved according to predicted bank retreat

5 Results and Discussion

Simulations have been carried out for the period of April 2009 through August 2011 under the existing condition for model calibration and verification purpose. The study also serves to understand what a 2D model can do in modeling gravel bed streams with riffles and pools.

5.1 Baseline Model Results

A baseline model is identified so that other model results may be compared to it. The baseline model has the following model inputs:

(1) The sediment transport capacity equation is based on the Trinity equation as shown in equations (10) to (12);
(2) The adaptation length is based on that derived from Seminara equations as in equation (6d); and
(3) There are no bed slope corrections to the critical or reference shear stress used by the capacity equation.

The baseline model results are presented first in this section while other model results are discussed in the next section.

The net erosion and deposition depth between April 2009 and August 2011 based on the survey data is shown in Figure 17. The data suggested that the three pools, marked as "Pool 1," "Pool 2" and "Pool 3" in Figure 17, were subject to a small amount of deposition while a section of the left bank, marked as "Bank Erosion" in Figure 17, experienced significant bank erosion. We would like to investigate what a 2D geofluvial model such as SRH-2D can accomplish in modeling gravel rivers such as the Trinity River. It has been known (e.g., Logan et al. 2010) that the sediment transport and morphologic modeling of riffle-pool systems is very challenging with any numerical models while few existing morphological models can be used to simulate lateral bank erosions.

Two baseline model runs were carried out: one without the use of bank erosion module (named No-Bank-1) and another with the bank erosion module (named With-Bank-1). The predicted net erosion and deposition are compared with the measured data in Figure 18 and Figure 19; zoom-in views of the same plots are displayed in Figure 20. In addition, the predicted bed elevation changes in time at the deepest points of Pool 1 and Pool 2 are plotted in Figure 21.

The model results show that bank erosion on the left cannot be predicted with the No-Bank-1 case; bank erosion module needs to be activated. The With-Bank-1 run is capable of predicting bank erosion on the left channel by simply using the

measured and BSTEM estimated bank parameters. No attempt of changing the critical shear stress or erodibility has been made to improve the model prediction of the bank retreat rate.

A comparison of No-Bank-1 and With-Bank-1 results show that the eroded bank sediments are mostly deposited in the stream near the eroded bank and they are not transported to downstream appreciably during the simulation period. More than 50% of the eroded bank sediments are large gravels and small cobbles at UJC-E and UJC-F and they are less movable once deposited in the stream. As a result, the impact of the eroded bank sediments on the downstream reach is relatively small.

Upstream of the bank erosion zone, both No-Bank-1 and With-Bank-1 runs are capable of predicting the overall erosion and deposition patterns. The differences in results of the two runs are relatively small in the upstream reach. Therefore, the No-Bank model runs may be used to assess the model capability to predict the riffle-pool processes at this site.

There are two main discrepancies between the model prediction and the measurement. First, the model predicted much more deposition than the measurement in the three pools. Second, the riffle erosion downstream of Pool 2 is not predicted by the model. The predicted bed elevation changes at the deepest points of the first two pools are plotted in Figure 21. A total of 5 and 8 feet of deposition are predicted in Pool 1 and 2, respectively; the corresponding measured depositions are approximately 2.2 and 3.2 feet. Over-prediction of the pool filling process has been a consistent problem of any depth averaged numerical models since such models do not take the horizontal vortices into consideration. 3D models may have the potential to improve the predictions; but they are yet to be demonstrated. Other factors may also contribute to the poor prediction of the pool filling process. High uncertainty in the initial bed gradation specification of the riffle areas is one of the causes. Over-prediction of erosion at riffles may lead to increased deposition in the downstream pool. Sediment transport capacity equations are the other weak links in predicting the riffle-pool systems as most existing ones are based on reach-averaged or depth-averaged variables.

Riffle erosion downstream of Pool 2 is predicted after the first two-year runoffs (2009 and 2010) as shown in Figure 18a and Figure 19a; it is not predicted, however, in August 2011. The reason for the failure of the numerical model in predicting the riffle erosion in this area is unclear. It may be caused by factors such as an inaccurate bathymetry, uncertainty in bed gradation, neglect of bank vegetation impact, and/or too much upstream sediment supply at higher discharges. We believe the most probable cause is the existing mature trees along the nearby right bank which is under water only at high discharges that occurred in 2011.

Downstream of the bank erosion zone, model results are less accurate since the downstream stage-discharge rating curved used may have a large impact on the predicted results. There is no measured net erosion and deposition data near the downstream boundary so it is difficult to assess.
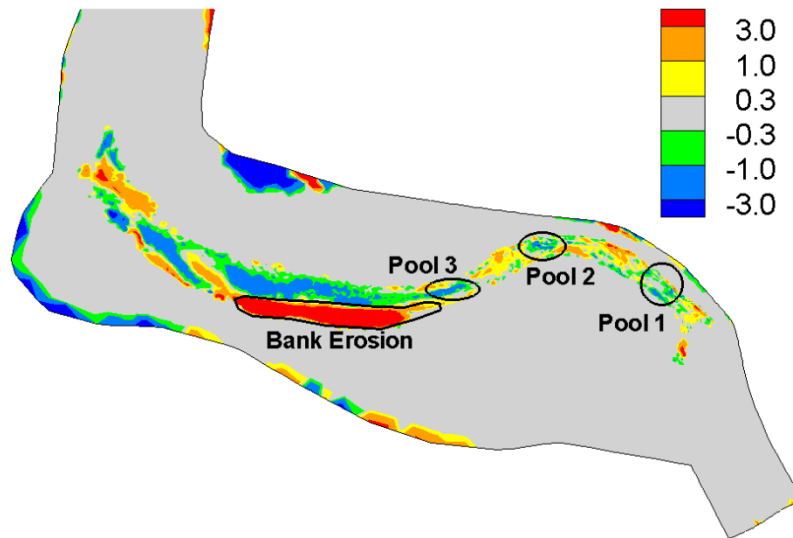

Figure 17. Measured net erosion (positive) and deposition (negative) depth (feet) between April 2009 to August 2011
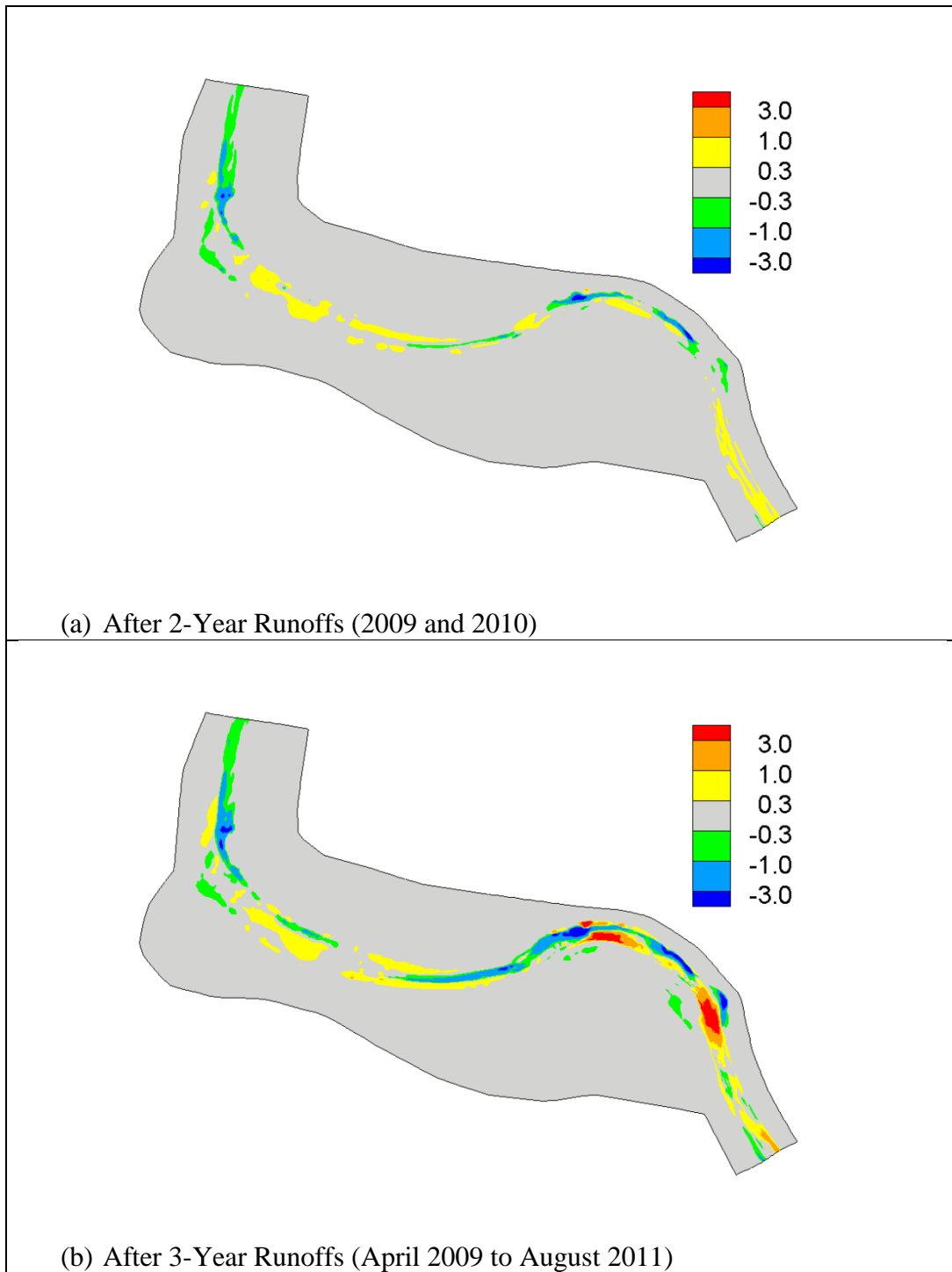
(a) After 2-Year Runoffs (2009 and 2010)

(b) After 3-Year Runoffs (April 2009 to August 2011)

Figure 18. Predicted net erosion (positive) and deposition (negative) depth in feet with the No-Bank-1 case

(a) After 2-Year Runoffs (2009 and 2010)

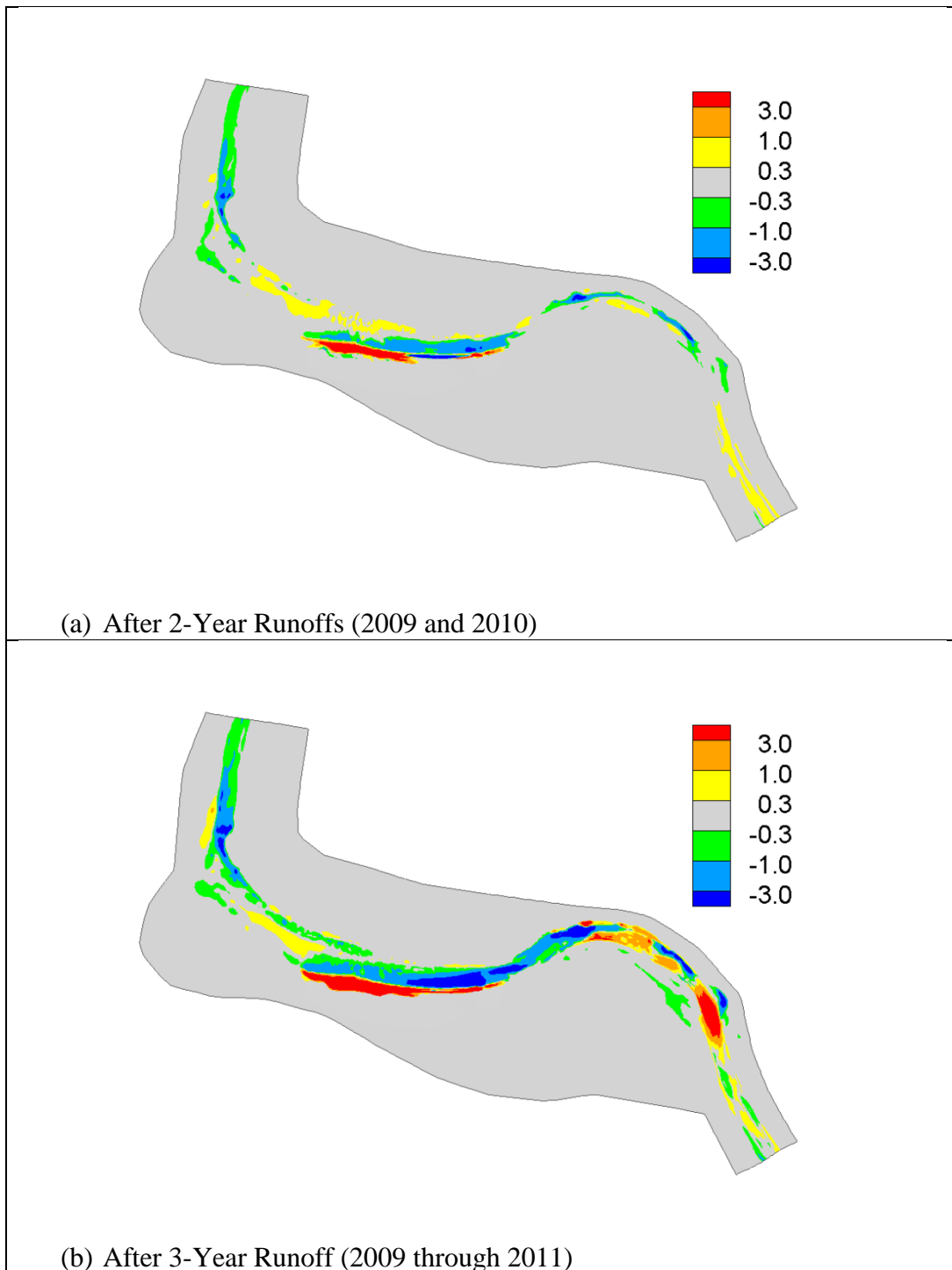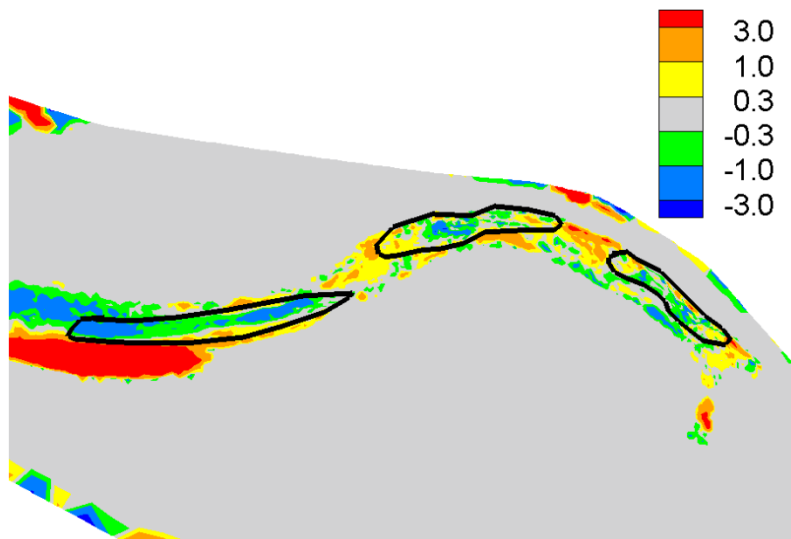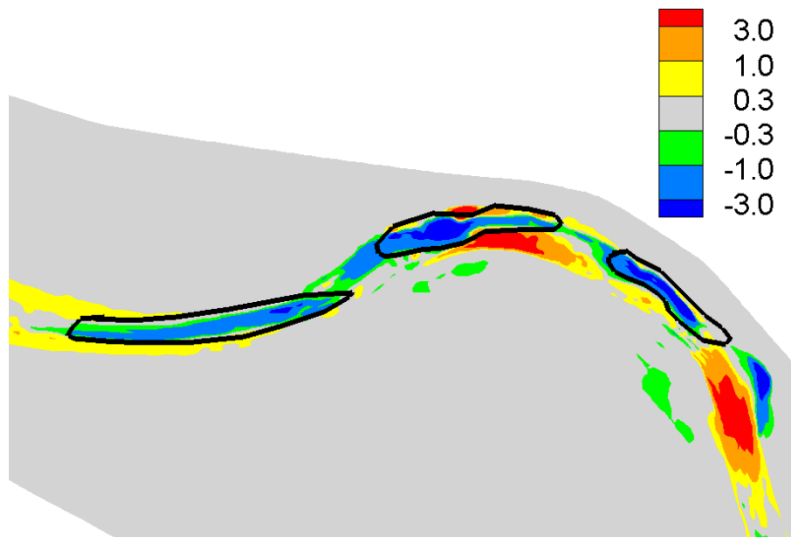(b) After 3-Year Runoff (2009 through 2011)

Figure 19. Predicted net erosion (positive) and deposition (negative) depth in feet with the With-Bank-1 case

(a) Measured Data

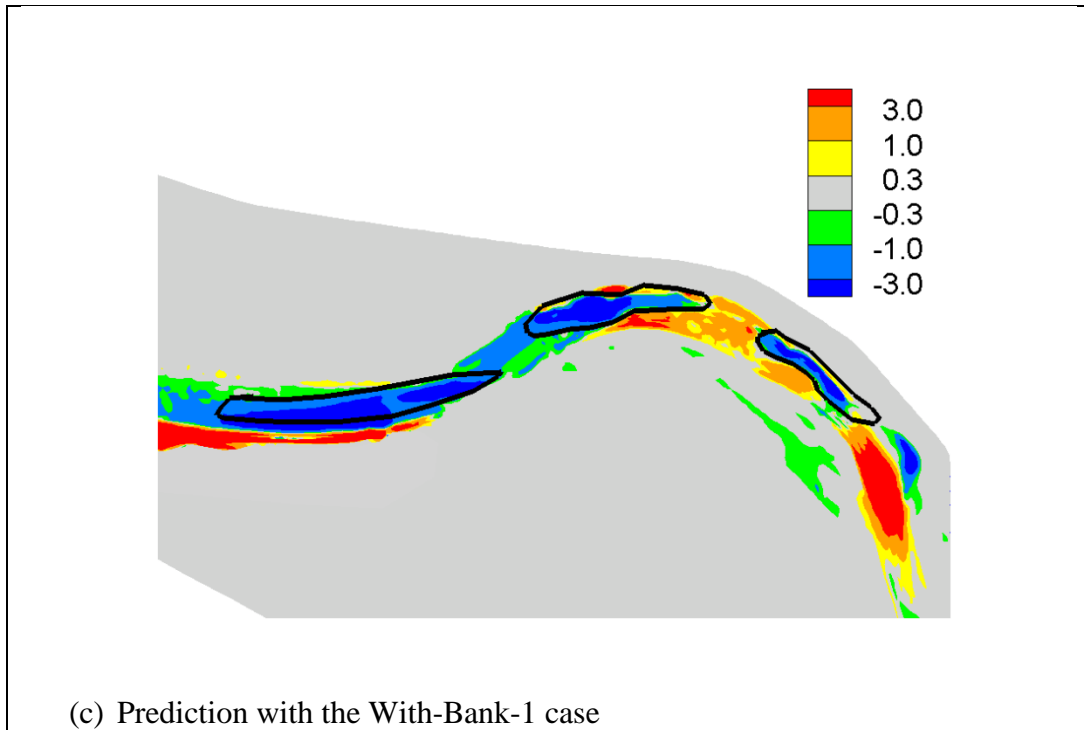(b) Prediction with the No-Bank-1 case

(c) Prediction with the With-Bank-1 case

Figure 20. Zoom-in views of the predicted and measured pool-filling after 3-year runoffs (2009 through 2011)

(a) Prediction with the No-Bank-1 case

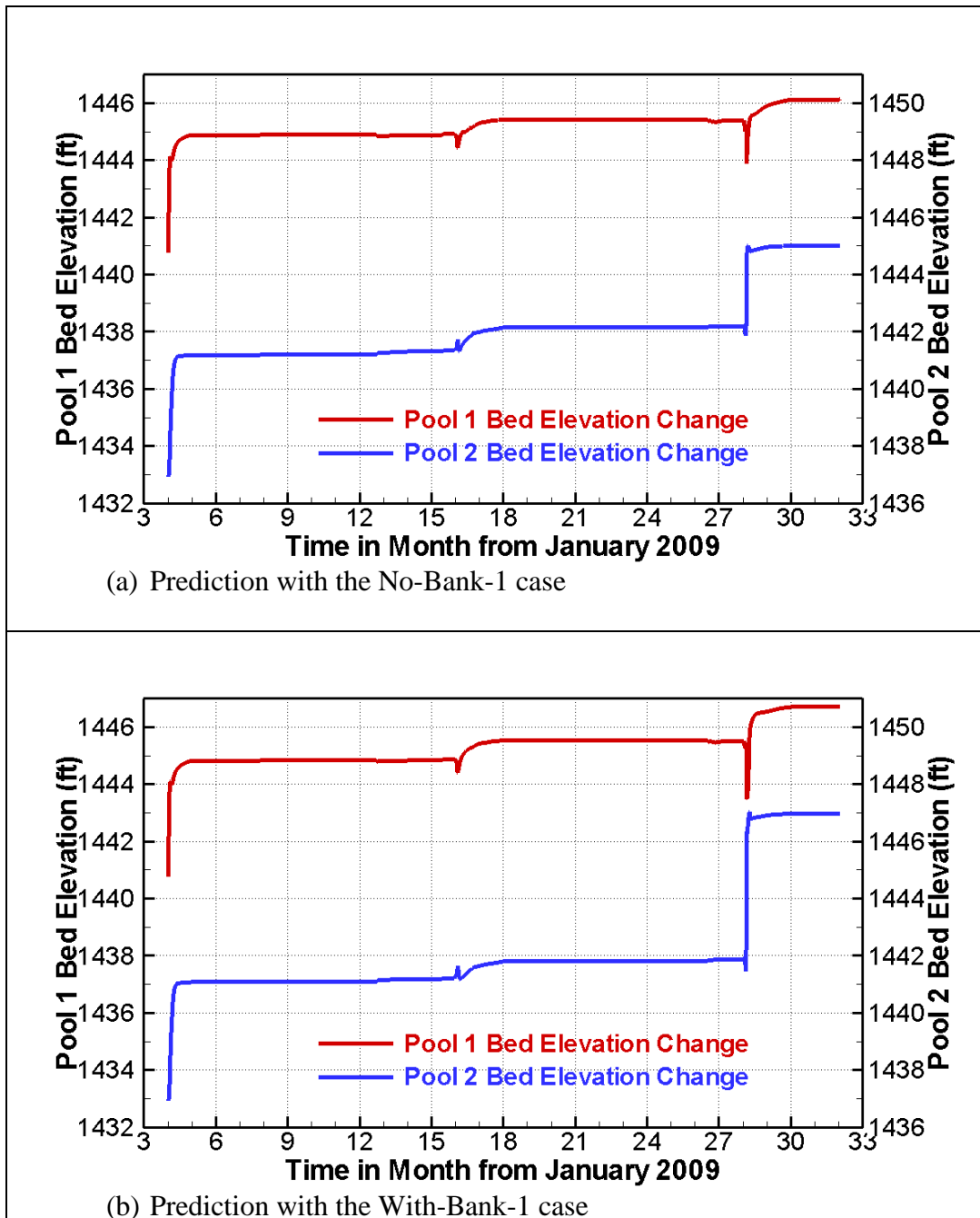(b) Prediction with the With-Bank-1 case

Figure 21. Predicted bed elevation variations in time at the deepest points of Pool 1 and Pool 2

5.2 Sensitivity Study of the No-Bank Cases

Sensitivity studies have been carried out using the No-Bank model since the difference between the No-Bank and With-Bank runs is small in predicting the riffle-pool processes upstream of the bank erosion zone.
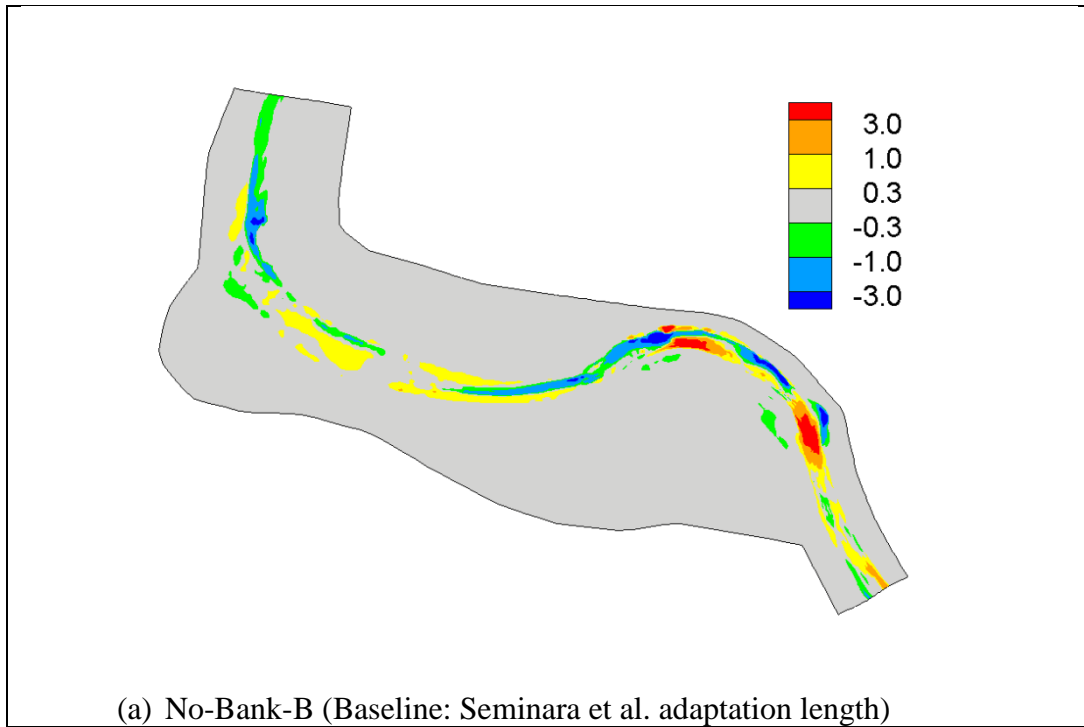
Sediment transport capacity equations and bedload adaptation length are two of the most important empirical parameters for morphological modeling in streams. The capacity equation provides the erosion potential by a non-equilibrium model; it is not the actual sediment transport rate in streams as the equilibrium models. The adaptation length quantifies the travel distance required for a packet of sediment to reach a new equilibrium concentration when it moves into a region of higher or lower shear stress. A number of sensitivity studies have been carried out with regard to these two parameters.

Three cases are simulated with regard to the different adaptation length equations. They are named No-Bank-B, No-Bank-A2, and No-Bank-A3. All three cases use the Trinity capacity equation but with different adaptation length equations. No-Bank-B is the baseline model run that uses the Seminara equation in (6d); No-Bank-A2 adopts the constant adaptation length of 80 meters that is about 2.5 times the average channel width; No-Bank-A3 utilizes equation (7). The model results of the three cases are shown in Figure 22.. The model results show that the differences between the No-Bank-B and No-Bank-A2 are insignificant; however, the use of equation (7) with the No-Bank-A3 case leads to appreciable changes particularly in the reach upstream of the pools. More deposition is predicted with No-Bank-A3.

Three additional cases are compared with regard to the use of different transport capacity equations. They are named No-Bank-B, No-Bank-C2, and No-Bank-C3. No-Bank-B is the baseline model run that uses the Trinity capacity equations in (10) to (12); No-Bank-C2 uses the Seminara et al. (2002) entrain and deposition rates equations in (4) and (5); and No-Bank-C3 uses the Wilcock-Crowe (2003) equation. The results with the Seminara et al. (2002) equations are found to be unrealistic since they lead to significantly high erosion over the entire channel. Therefore, No-Bank-C2 results presented below are based on the run with a much smaller α coefficient of 0.00199 (the original equation used 0.0199). The model results of these three cases are shown in Figure 23. It is seen that the Seminara et al. capacity equation predicts similar net erosion and deposition results as the Trinity capacity equation only after a factor of 10 reduction in the computed capacity. Therefore, the Seminar et al. capacity equation may not be adequate in predicting the bedload transport for the Trinity River. The Wilcock-Crowe capacity equation produced too much erosion in the channel and the results do not seem to be reasonable. It is noted that the use of higher sediment capacity rate increases the erosion but the pool-filling is still over-predicted. It may suggest that pool-filling feature cannot be predicted well if the same capacity equation is applied over both net deposition and erosion zones. Different pickup rate

(capacity) equations or adaptation length equations may be needed in erosion and deposition zones.

Finally, the bed slope dependent reference critical shear stress equations in (8) and (9) are used to simulate the case. The two cases, No-Bank-B and No-Bank-S, are compared in Figure 24 to understand the effect of slope dependent reference shear stress on the model results. The No-Bank-S run is the same as No-Bank-B except for the use of equations of (8) and (9). The results show that the impact of the slope-dependent critical shear stress of equations (8) and (9) on the model results is negligible in most areas while a slight improvement is observed in the prediction near Pool 1 and Pool 2.

(a) No-Bank-B (Baseline: Seminara et al. adaptation length)

(b) No-Bank-A2 (Constant adaptation length of 80 m)
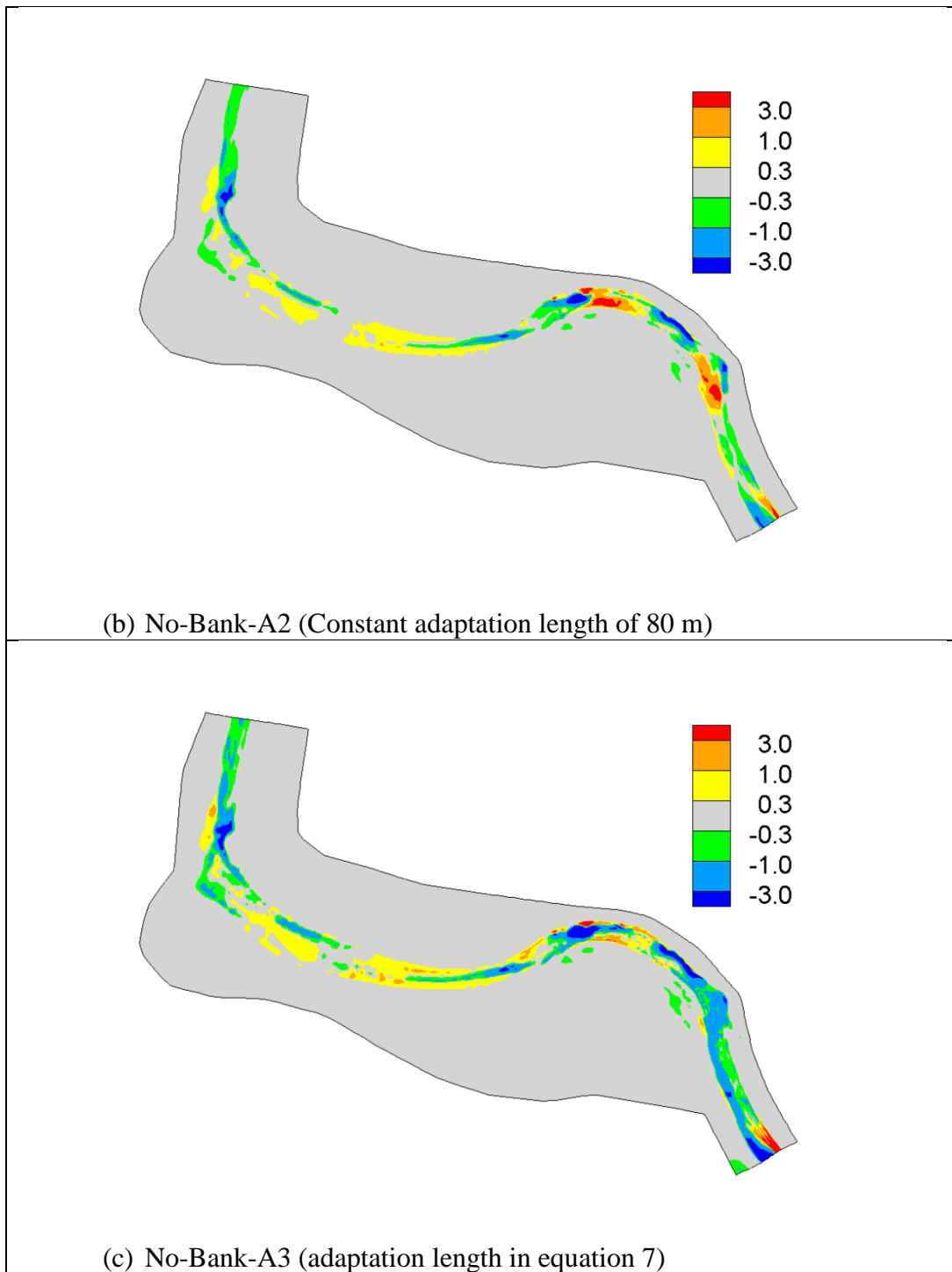

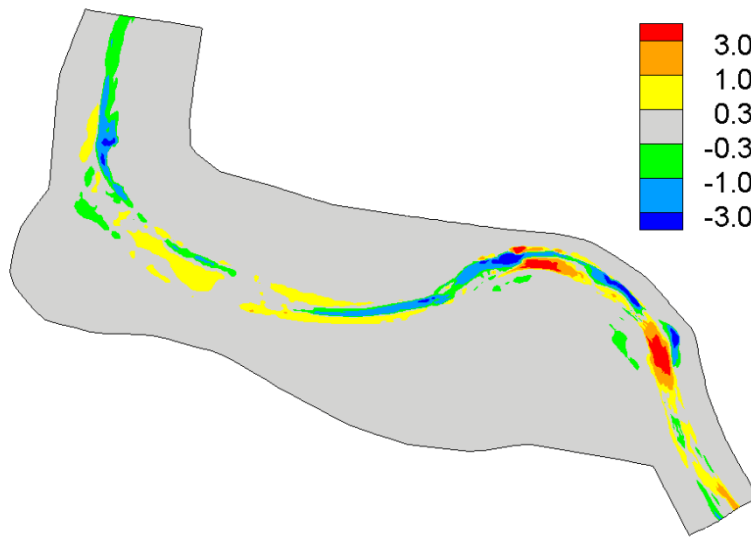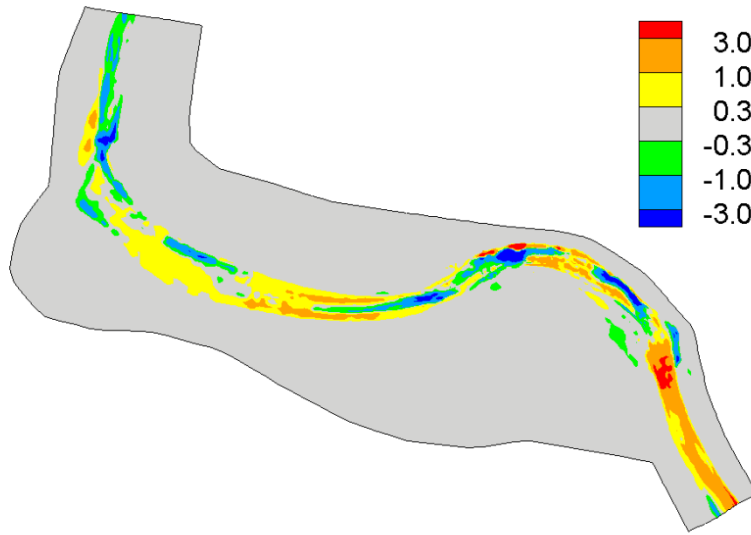(c) No-Bank-A3 (adaptation length in equation 7)

Figure 22. Sensitivity of the predicted net erosion (positive) and deposition (negative) depth in feet to the adaptation length equations

(a) No-Bank-B (Trinity Capacity Equation)
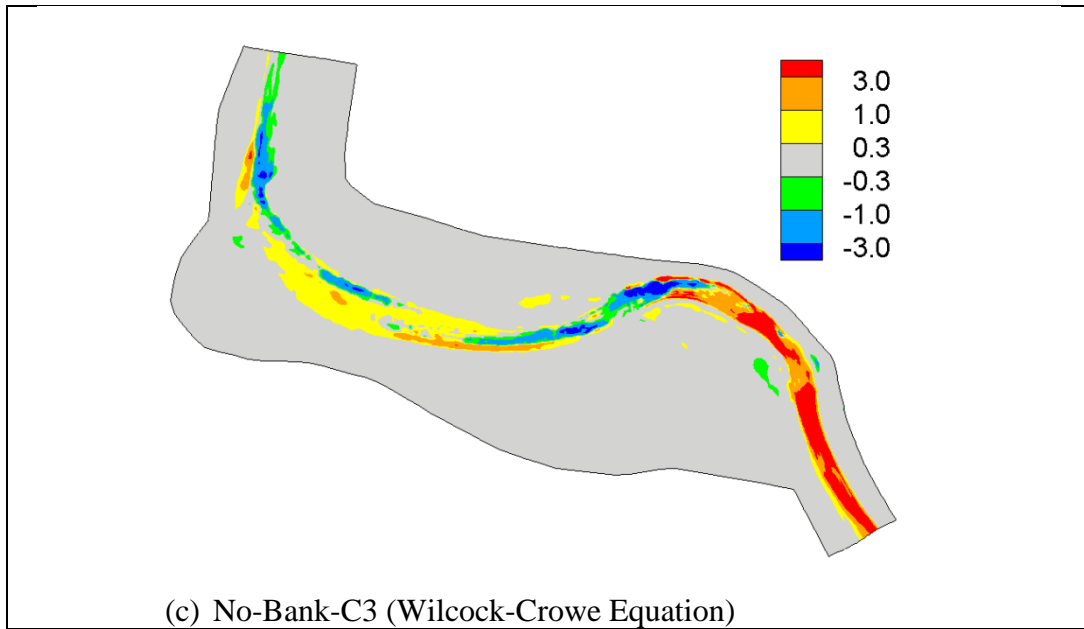

(b) No-Bank-C2 (Seminara et al. Equation)

(c) No-Bank-C3 (Wilcock-Crowe Equation)

Figure 23. Sensitivity of the predicted net erosion (positive) and deposition (negative) depth in feet to the sediment transport capacity equation

(a) No-Bank-B (flat-surface reference shear stress)

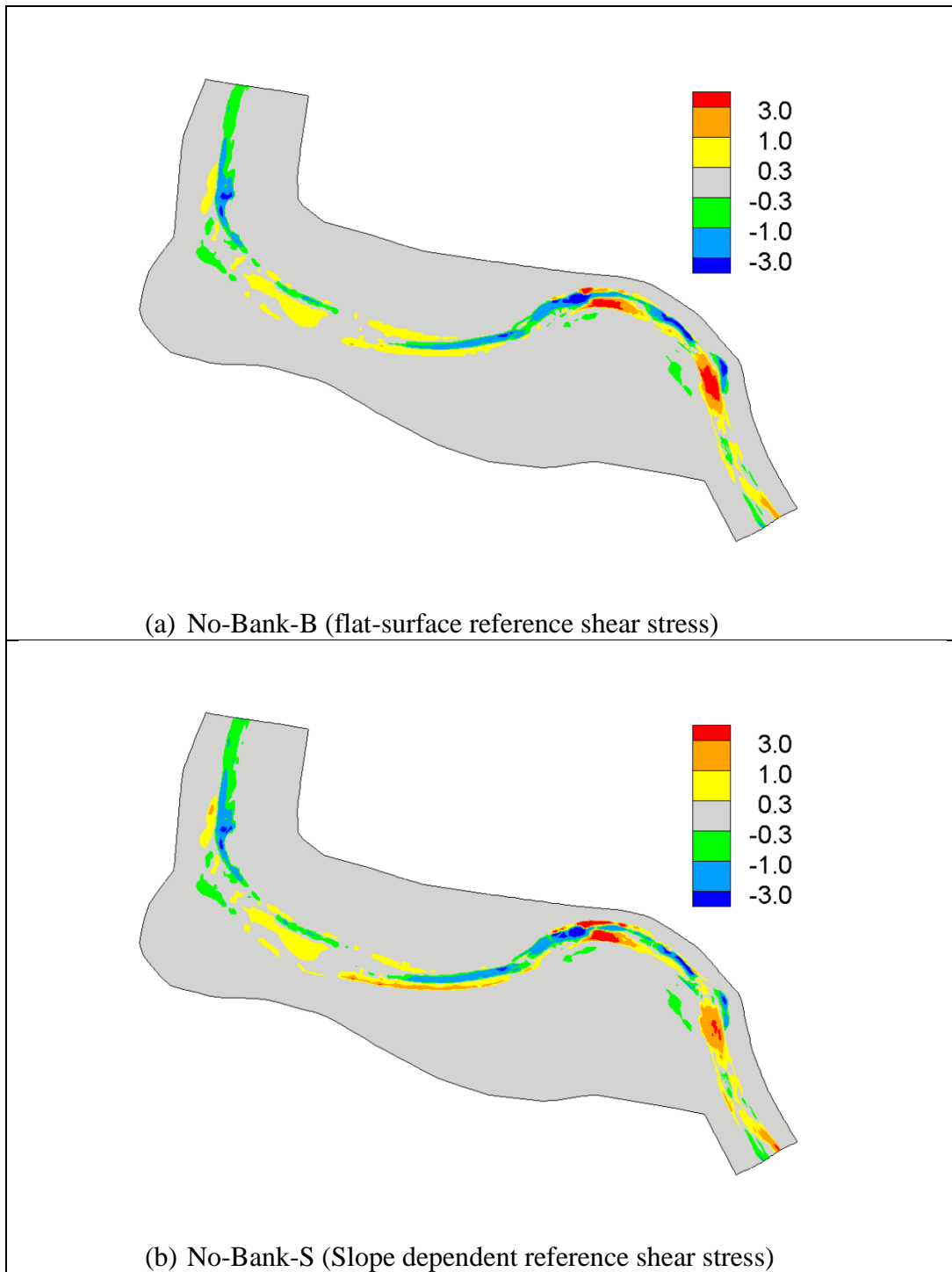(b) No-Bank-S (Slope dependent reference shear stress)

Figure 24. Sensitivity of the predicted net erosion (positive) and deposition (negative) depth in feet to the slope dependent reference shear stress

6 References

Armanini, A. 1992. Variation of bed and sediment load mean diameters due to erosion and deposition processes, In Dynamics of gravel-bed rivers, P. Billi, R.D. Hey, C.R. Thorne, and P. Tacconi, eds. John Wiley and Sons, pp. 352-359.

Armanini, A. and G. Di Silvio, 1988, A one-dimensional model for the transport of a sediment mixture in non-equilibrium conditions, Journal of Hydraulic Research, 26(3):275-292.

Cardno ENTRIX. (2012). *Bank-Stability Analysis of the Upper Junction City Reach Trinity River, CA*, Project Report by Cardno Entrix, Project 30088130, December, 2012.

Gaeuman, D., Andrews, E.D., Krause, A., and Smith, W. (2009). "Predicting fractional bed load transport rates: Application of the Wilcock-Crowe equations to a regulated gravel bed river," Water Resour. Res., 45, W06409, doi:10.1029/2008WR007320.

Greimann, B., Y. Lai and J. Huang, 2008, Two-dimensional total sediment load model equations, Journal of Hydraulic Engineering, 134(8):1142-1146.

Iervoino, M., M. Pontillo, and C. Di Cristo. 2010. Comparison among different entrainment/deposition functions in the simulation of a 1D dam-break. In River Flow 2010, A. Dittrich, Ka. Koll, J. Aberle, and P. Geisenhainer, eds., Bundesanstalt für Wasserbau, Karlsruhe, Germany.

Lai, Y.G., Weber, L.J., and Patel, V.C. (2003). "Non-hydrostatic three-dimensional method for hydraulic flow simulation - Part I: formulation and verification," J. Hydraul. Eng., ASCE, 129(3), 196-205.

Lai, Y.G. and Randle, T.J. (2007). *Bed Evolution and Bank Erosion Analysis of the Palo Verde Dam on the Lower Colorado River*. Technical Service Center, Bureau of Reclamation, Denver, CO.

Lai, Y.G. (2008). *SRH-2D Theory and User's Manual version 2.0,* Technical Service Center, Bureau of Reclamation, Denver, CO.

Lai, Y.G. and Greimann, B.P. (2008). "Modeling of erosion and deposition at meandering channels," World Environmental & Water Resources Congress, ASCE, May 12-16, 2008, Honolulu, Hawaii.

Lai, Y.G. (2010). "Two-Dimensional Depth-Averaged Flow Modeling with an Unstructured Hybrid Mesh," *J. Hydraulic Engineering*, ASCE, 136(1), 12-23.

Lai, Y.G. and Greimann, B.P. (2010). "Predicting contraction scour with a two-dimensional depth-averaged model," *J. Hydraulic Research*, IAHR, 48(3), 383-387.

Lai, Y.G., Greimann, B.P., and Wu, K. (2011). "Soft bedrock erosion modeling with a two-dimensional depth-averaged model," *J. Hydraulic Engineering*, ASCE, vol.137(8), pp.804-814.

Logan, B., Nelson, J., McDonald, R., and Wright, S. (2010). "Mechanics and Modeling of Flow, Sediment Transport and Morphologic Change in Riverine Lateral Separation Zones," 2nd Joint Federal Interagency Conference, Las Vegas, NV, June 27 - July 1, 2010.

Parker, G., G. Seminara, and L. Solari, 2003, Bed load at low Shields stress on arbitrarily sloping bed: Alternative entrainment formulation, Water Resources Research, 39(7),1183, doi:10.1029/2001WR001253.

Rahuel, G.T., F.M. Holly, J.P. Chollet, P.J. Belleudy, and G. Yang, 1989, Modeling of riverbed evolution for bedload sediment mixtures, Journal of Hydraulic Engineering 115(11):1521-1542.

Seminara, G., L. Solari, and G. Parker, 2002, Bed load at low Shields stress on arbitrarily sloping beds: Failure of the Bagnold hypothesis, Water Resources Research, 38(11), 1249, doi:10.1029/2001WR000681.

van Rijn, L.C., 1984, Sediment transport, part III: Bed forms and alluvial roughness, Journal of Hydraulic Engineering 110(12):1733-1754.

Wilcock, P.R. and Crowe, J.C. (2003). "Surface-Based Transport Model for Mixed-Size Sediment," J. Hydraulic Engineering, 129: 120-128.

Wu, W., W. Rodi, and T. Wenka, 2000, 3D numerical modeling of flow and sediment transport in open channels, Journal of Hydraulic Engineering, 126(1):4-15.

Wu, W., 2004, Depth-averaged two-dimensional numerical modeling of unsteady flow and nonuniform sediment transport in open channels, Journal of Hydraulic Engineering, 130(1): 1013–1024.

Wang, S.S.Y. and W. Wu, 2004, River sedimentation and morphology modeling – the state of the art and future development, Proceedings of the Ninth International Symposium on River Sedimentation, Oct. 18-21, 2004, Yichang, China.

Wu, W., D.A. Vieira, and S.S. Wang, 2004, A 1-D numerical model for nonuniform sediment transport under unsteady flows in channel networks, Journal of Hydraulic Engineering, 130(1): 1013–1024.